Dividing Lines: Racial Segregation across Local Government Boundaries*

Tomás Monarrez   David Schönholzer

December 31, 2021

Abstract

We describe the empirical relationship between local government boundaries and residential segregation in the US. First, we study recent changes in the distribution of segregation within and between local governments in metropolitan areas, using census block data on residential demographics over the period 1990-2020. We find that segregation across local government boundaries explains a substantial share of racial stratification patterns in metropolitan areas, which has changed only little over the last thirty years. Next, we use spatial regression discontinuity methods to distinguish between household sorting due to neighborhood amenities and public goods provided by local governments. The prevalence of demographic discontinuities at local government boundaries suggest that between-jurisdiction segregation patterns cannot be explained solely by proximity to neighborhood amenities. We discuss implications for policy and future research, showing that both between-jurisdiction segregation and jurisdictional discontinuities can partly explain the correlation between total segregation and racial gaps in educational outcomes.

1 Introduction

Segregation on the basis of race and ethnicity is one of the most enduring and widespread social problems in American cities. A large literature has established the harms of racial segregation, especially for individuals of color (Guryan, 2004; Card and Rothstein, 2007; Boustan, 2010; Billings et al., 2014). In economics, most research on the determinants of segregation focuses on individual choices and residential sorting behavior (Cutler et al., 1999; Bayer et al., 2004, 2007; Card et al., 2008; Baum-Snow and Lutz, 2011; Caetano and Macartney, 2021). However, a burgeoning literature both in economics and in related fields documents the historical role of government institutions and policies in determining and perpetuating segregation (Shertzer et al., 2016; Akbar et al., 2019; Li, 2021).

The goal of this paper is to shed light on the role of local government boundaries in enabling segregation. Local government constitutes the central body through which many public goods are provided and regulatory policies are implemented. Most US metropolitan areas are broken up into dozens of sub-units, both jurisdictional (e.g. city governments and school districts) and administrative (e.g. land-use zoning regulations and school attendance boundaries). At the same time, across both cities and school districts, there are often enormous differences in the quality of public goods provided by different local governments, even when they neighbor each other. For example, emergency response times are more than twice as long in Oakland, CA than in neighboring Piedmont, and average teacher salaries in its school district are more than 15% lower.[1]

We provide comprehensive evidence on the contribution of local government boundaries to racial inequality across urban areas in the United States using two approaches. In the first approach, we unify and extend recent attempts to decompose segregation into variation between and within local governments (Clotfelter, 1999; Trounstine, 2018). Drawing together census block data for all 380 metropolitan areas (MAs) and thousands of local government boundaries for cities, school districts, and counties over thirty years, we can study the recent evolution of segregation in new light. Given the increasing racial and ethnic diversity of the US population, we compute total segregation and segregation between local government jurisdictions for Black, Hispanic, and Asian residents.[2]

This approach establishes several novel insights into the nature of segregation in urban America. First, while segregation for Black residents has fallen substantially between 1990 and 2020, this is almost entirely due to a drop in segregation within jurisdictions as opposed to between jurisdictions. This means that while segregation today is lower than at any point in the last thirty years, access

---

[1]Emergency response times for Oakland are here; Piedmont response times per public records request. Teacher salaries for all California districts are here.

[2]To be specific, we use the following census categories of minorities: non-hispanic Black residents (which we refer to as Black residents for simplicity), Hispanic residents of all races (henceforth simply Hispanic residents), as well as Asian and Pacific Islanders (henceforth simply Asians).

to public goods has hardly become more equitable over this period. Second, the drop in segregation of Black residents within jurisdictions is almost entirely driven by lower segregation in the most severely segregated jurisdictions; indeed, the median city and school district are no less segregated today than thirty years ago. Third, both total segregation and segregation between jurisdictions has been on the rise for both Hispanic and Asian residents. This is true despite the gradual expansion of these groups from a few large MAs across all urban areas.

In the second approach, we zero in on neighborhoods near local government boundaries to estimate to what extent demographics change discontinuously near these boundaries across space, and how these changes evolved across time. To interpret these demographic discontinuities, we develop a model of household sorting, in which households value both neighborhood amenities and public goods. This model establishes that discontinuities do not only emerge if preferences for public goods differ by group, but also if groups have differential access to public goods or if there is price discrimination in the housing market.

Empirically, we find that, on average, there are substantial discontinuities across boundaries for all three racial/ethnic groups. These discontinuities tend to be larger near city boundaries than school district boundaries, perhaps reflecting the capacity of cities to control land-use zoning. Together, the evidence presented here suggests that local government boundaries play a central role in household sorting, access to public goods, and persistent residential segregation.

1.1 The New Economic Literature on Segregation

These findings connect to a large economics literature on segregation. The canonical literature stems from the economic tradition of studying the constrained optimization problem faced by households, in this case in their choice of residential location. Dating back to the work of Tiebout (1956) and Schelling (1971), the primitive determinant of sorting in models of location choice has been heterogeneity in the preferences of individuals. While governments are not entirely absent in some of these models, their role is passive, often one of a benign social planner concerned with maximizing a social welfare function when setting public good provision.

Empirical work on neighborhood segregation has imposed similar assumptions when estimating structural models of residential choice. For example, the standard framework in the work by Dennis Epple and coauthors (Epple et al., 1978, 1984, 1993; Epple and Platt, 1998; Epple and Sieg, 1999; Epple et al., 2001; Calabrese et al., 2012) models residential location as the outcome of a model with a second stage involving the public choice of a bundle of public goods within a jurisdiction (the chosen bundle is the one preferred by the median voter), and a first stage with households choosing which jurisdiction to live in. Government here is simply represented as a tool for aggregating preferences. Other empirical work has leveraged advances in the estimation of discrete choice

models to make inferences of the same spirit (Bayer et al., 2007). When jurisdictional differences in public good provision have been documented, they have been attributed directly to heterogeneity in "willingness to pay" across households of different characteristics (Black, 1999; Boustan, 2012).

While preference heterogeneity is clearly a driver of segregation, equilibrium residential segregation is also determined by constraints imposed by governments. Earlier work has looked at this issue, concluding that preferences are much more important than constraints. Barriers to access better neighborhoods and schools are seen as a phenomenon of the past, which over time were replaced by market forces. For example, (Cutler et al., 1999, p. 496) write that "[d]ecentralized racism operating through the price mechanism has replaced centralized, legally enforced racism, and racial differences in housing persist."

In contrast, a new economic literature on segregation establishes that government policies actively shaped segregation. Aaronson et al. (2020, 2021) show that the 1930s HOLC "redlining" maps had important impacts on the long run trajectories of cities, reducing homeownership rates, house values, and rents and increased racial segregation in later decades. Avenancio-León and Howard (2019) establish that racial inequality in governments' assessment of property values has resulted in Black and Hispanic residents facing a higher tax burden for the same bundle of public services. In an investigation of the causal drivers of segregation in Los Angeles during the 1940s, Li (2021) concludes that constraints on which neighborhoods Black households can access matter more than preferences in explaining segregation. This work signals a change in economic thought in recent years. Government is no longer seen as neutral, instead conceptualized as controlled by a faction of the population, serving their interests and potentially exacerbating inequality.

In a similar vein, a new literature explores the motive and impact of land use regulation on social inequality. Shertzer et al. (2016) study the causes of land use regulation in Chicago, finding that industrial zoning was disproportionately allocated to neighborhoods populated by racial minorities. Trounstine (2018) argues that the intent of land use zoning often was to create segregation by design. While land use regulation was once considered the "trick" that saved Tiebout equilibrium, economists now question whether these regulations create inefficiencies that exacerbate inequality Hsieh and Moretti (2019); Ganong and Shoag (2017). More recent research has also established that influxes of Black residents during the Great Migration led to changes to municipal policy that was hostile to them, both in policing Derenoncourt (2018) and land use zoning Sahn (2021).

Our description of the empirical link between segregation and local government boundaries provides important context for the mechanisms documented by the new economic literature on segregation. Strategic boundary setting may have played a central role in enabling local governments to segregate urban spaces, and boundary changes may play an important part in policy to reduce segregation. However, boundary setting involves different procedural rules and has different

implications across different types of local governments. We provide a brief description and history of relevant local government types and the processes that determine their geography in Appendix B.

2 Decomposing Segregation Across Jurisdictions

While the new literature on segregation recognizes the role of government in shaping residential segregation throughout history, economists lack a comprehensive framework to quantify the relationship of local government boundaries with segregation today. Our first approach to doing so is to decompose measures of segregation into a neighborhood component and a local government component. To be clear, such a decomposition cannot speak to the causal role of government in segregation. However, it yields new facts that take stock of government policy in determining access to high-quality public goods.

We are not the first to decompose segregation into neighborhoods and local governments. Clotfelter (1999) studied school segregation within metropolitan areas in 1990, distinguishing between racial disparities within and between school districts. Trounstine (2018) investigates residential segregation between and within cities using a similar approach. We extend this decomposition idea to include cities, counties, and school attendance zones for Black, Hispanic and Asian residents and all decades between 1990 and 2020.

We use census block data for all decennial censuses between 1990-2020 for the four largest racial/ethnic groups: White, Hispanic (of all races), Black, and Asian. These demographic data are combined with all local government boundaries from Census TIGER/Line products for corresponding years. More details on the data are described in Appendix A.

2.1 Measuring Segregation

There is a long tradition in the social sciences of quantifying segregation. We rely primarily on the "eta-squared" index, which has become widely used in economics since Kremer and Maskin (1996), with a much longer history in other social sciences (e.g. Duncan and Duncan 1955). Graham (2018) discusses many of the convenient features of this index. We show below that it can be decomposed into neighborhood variation within and variation between jurisdictions, which allows us to separately quantify the role of local government divisions and neighborhood sorting. This refinement of the eta-squared index provides a rich picture of how the spatial distribution of groups across neighborhoods and across space more generally relates to the location of jurisdictional boundaries.

Consider a metro area divided into J *jurisdictions*, such as school districts or cities. Each jurisdiction $j = 1, ..., J$ has I_j *neighborhoods* indexed by $i = 1, ..., I_j$. The population in neighborhood i

4

of jurisdiction j has population N_{ij}, of which M_{ij} are minorities, such as Black or Hispanic people. Let $m_{ij} = M_{ij}/N_{ij}$ be the corresponding minority share. Total and minority populations aggregate to jurisdiction j as $N_j = \sum_{i=1}^{I_j} N_{ij}$ and $M_j = \sum_{i=1}^{I_j} M_{ij}$, respectively, with minority share $m_j = M_j/N_j$. Altogether, the metro area is home to $N = \sum_{j=1}^{J} N_j$ people, of which $M = \sum_{j=1}^{J} M_j$ are minorities, such that the minority share is $m = M/N$.

2.2 Neighborhood Segregation Within Jurisdictions

The *isolation index θ_j of jurisdiction j* describes the average minority share in the neighborhood *of minorities* in j. Unlike the minority share m_j, it captures the minority share not for all people in j but only for minorities. In this sense, it measures how isolated a minority group is from other groups. It is defined as

$$\theta_j = \sum_{i=1}^{I_j} \frac{M_{ij}}{M_j} m_{ij},$$

where weights M_{ij}/M_j are the share of minorities in j that live in neighborhood i with $\sum_{i=1}^{I_j} M_{ij}/M_j = 1$. If the jurisdiction were perfectly integrated and minorities were evenly distributed across neighborhoods, each neighborhood would have a minority share of exactly $1/I_j$ in the jurisdiction, making isolation equal the minority share: $\theta_j = m_j$. In contrast, were the jurisdiction perfectly segregated such that minorities lived in neighborhoods that were entirely minority, then the minority share in those neighborhoods would be $m_{ij} = 1$ with positive weights M_{ij}/M_j, and the minority shares and weights in other neighborhoods would be zero. Since $\sum_{i=1}^{I_j} M_{ij}/M_j = 1$, we would then have an isolation index of $\theta_j = 1$: minorities are completely isolated from other people, with every minority living in a 100% minority neighborhood.

While the isolation index is bounded from above by one, it can only be as low as the minority share in the jurisdiction, and so jurisdictions with a higher minority share automatically have a higher isolation index. It is thus convenient to rescale the isolation index to account for this mechanical relationship between minority share m_j and isolation index θ_j. This is exactly what the *segregation index of jurisdiction j* does:

$$\eta_j^2 = \frac{\theta_j - m_j}{1 - m_j},$$

which is bounded between zero and one. This index measures how much more isolated minorities are in jurisdiction j than they would be if they were perfectly integrated (the numerator), relative to how much more isolated they would be in a counterfactual world of perfect segregation (the denominator).

We use the example of New York City (NYC) to illustrate these concepts. About 22% of

residents of NYC are Black, with most residing in and handful of neighborhoods across the city, as shown in Figure 1. If they were perfectly integrated by being evenly distributed across all neighborhoods, Black residents (and everyone else) would be exposed to a Black neighborhood share of 22% everywhere, eliminating shade variation in Figure A.1. In this case, the isolation index would be $\theta_{\text{NYC}} = 0.22$, and segregation would be $\eta_{\text{NYC}} = 0$. In contrast, if NYC were perfectly segregated such that Black residents lived in neighborhoods that were entirely Black, then the share of Black residents in those neighborhoods would be 100%. Black residents would be completely isolated from other races (i.e. $\theta_{\text{NYC}} = 1$) and consequently the segregation of Black residents would be $\eta^2_{\text{NYC}} = 1$.

In reality, Black isolation in NYC is 53% ($\theta_{\text{NYC}} = 0.53$) and segregation is $\eta^2_{\text{NYC}} = 0.40$. NYC is moderately segregated for Black residents. While Black residents of NYC live in neighborhoods that are 33% more Black than the Black share in the city overall, they are still slightly closer to a state of perfect integration ($\eta^2_{\text{NYC}} = 0$) than perfect segregation ($\eta^2_{\text{NYC}} = 1$). We can compute the same statistics for Hispanic and Asian populations. Hispanics make up about 28% of NYC, whereas their average neighborhood is 48% Hispanic, resulting in segregation $\eta^2_{\text{NYC}} = 0.27$. Asians make up about 16%, living on average in neighborhoods that are 39% Asian, and their segregation is also $\eta^2_{\text{NYC}} = 0.27$.

Table 1 summarizes the 2020 distribution of segregation of the four major racial and ethnic groups and for the three types of local governments we study: incorporated cities, school districts, and counties. Because these distributions have long right tails, the table reports the 10th, 50th, and 90th percentiles of each. Black, Hispanic, and Asian populations had approximate national median isolation levels of 0.13, 0.18, and 0.09 (respectively) in both cities and school districts. Median segregation levels range between 0.07 and 0.12 for all race groups and across both cities and districts. The median US city and school district has meaningful but modest levels of segregation, driven largely by the numerous cities and districts in the country with really few minorities (at the median, 2% Black, 5% Hispanic, and 1% Asian).

Looking at cities and districts in 90th percentile tells quite a different story. Relative to the median, they are an order of magnitude larger. They are also about three times as segregated compared to median. Black segregation in the 90th percentile is about 0.30 in both cities and school districts. For Hispanic and Asian residents it is about 0.24 and 0.18, respectively. It is clear that within-jurisdiction segregation is a particularly pernicious issue for large and urbanized cities and school districts.

Figure 2 explores the extent to which within-jurisdiction segregation has changed over the last thirty years, for each of the racial groups and jurisdictional types. With the exception of counties, median levels of segregation have changed relatively little since 1990. Notwithstanding, the long

6

right tail of the segregation distribution for Black residents has decreased substantially, while for Hispanic and Asian households it has increased.

2.2.1 Metropolitan Area Segregation

We can extend our measure of segregation to the scale of a metropolitan area encompassing many jurisdictions. To this end, we define the *metropolitan isolation index* as:

$$\theta = \sum_{j=1}^{J} \sum_{i=1}^{I_j} \frac{M_{ij}}{M} m_{ij} = \sum_{j=1}^{J} \frac{M_j}{M} \theta_j,$$

Metropolitan isolation is the weighted sum of jurisdiction-specific isolation indices with weights given by jurisdictions' minority population share. We can then define the *total segregation index as*:

$$\eta^2 = \frac{\theta - m}{1 - m}.$$

Figure 3 shows a map of the school districts that make up New York metropolitan area, consisting of 499 independent districts, including the New York City Department of Education and many more across the suburbs of the tri-state area. The map includes a scatter plot corresponding to population-weighted census block centroids, colored in terms of the block's majority racial group. From this scale, the segregation of the New York metropolitan area is visually more striking than that of the the city proper (shown in Figure 1), largely due to the numerous suburban districts that are nearly 100% white. In particular, a number of districts in Long Island are nearly entirely white and geographically adjacent to districts that are nearly 100% Black or Hispanic, suggesting that a role for district boundaries in driving metropolitan segregation.

The total share of Black residents in the New York metropolitan area is 16%, but their isolation is 49%. Black isolation is high in the New York metropolitan area since there are a handful of districts that are majority Black, and many which have almost no Black residents. Figure A.2 in the appendix demonstrates this point by a showing a heat map of districts' Black population share across the area. The resulting metropolitan Black segregation is $\eta^2 = 0.40$. Hispanic residents make up 25% of the metro area and live in neighborhoods that are 47% Hispanic, resulting in $\eta^2 = 0.29$, which is slightly higher than their segregation index in NYC.

How does segregation vary across metropolitan areas? Figure 4 presents four US maps of metropolitan areas weighted by population, and colored based on their level of Black segregation in 1990, 2000, 2010, and 2020. Geographic heterogeneity in both segregation levels and changes is substantial across the country's urban clusters. Across this thirty year period, Black households were least segregated in the West, relative to the rest of the country. Moreover, the most Black

segregated metropolitan areas in 1990 have become increasingly integrated, including Chicago, Detroit, and New York. Black segregation has also decreased substantially in the South.

Table 2 digs deeper into these descriptive results, by showing a list of the 20 most and least Black segregated cities in the country. The five most Black segregated metropolitan areas are in the Midwest (Detroit MI, Milwaukee WI, Chicago IL, Cleveland OH, and St Louis MO), followed by many in the South, including Birmingham AL, Jackson MS, Baton Rouge LA, and Mobile AL. Detroit is still the most segregated city in the country even though it has become increasingly less so. In the appendix, we provide a list of the most and least segregated metropolitan areas for Hispanic and Asian households (Tables A.2 and A.3).Table 3 shows mean levels of metropolitan segregation for all groups and years.

2.3 Segregation Between Jurisdictions

So far, we have focused on the demographic breakdown of census blocks as the basic unit of interest. However, the metropolitan segregation findings above suggest that it is important to think of jurisdictions themselves as the unit of interest. For example, we may be interested in how segregated Hispanic residents are across school districts within the New York metro area. To this end, we can define a *between-jurisdiction isolation index* as

$$\bar{\theta} = \sum_{j=1}^{J} \frac{M_j}{M} m_j,$$

which is bounded between the metropolitan minority population share m (perfect between-integration) and total metropolitan isolation θ (perfect between-segregation). It is equal to the metropolitan minority share if minorities are evenly distributed across jurisdictions, $M_j/M = 1/J$ for all j such that $\bar{\theta} = m$. At the other extreme, it equals total metropolitan isolation $\bar{\theta} = \theta$ when minorities are evenly distributed *across blocks within each jurisdiction* such that each jurisdiction is perfectly integrated: $m_j = \theta_j$ and hence $\eta_j^2 = 0$ for all j. As before, it is convenient to rescale between-jurisdiction isolation so that it is bounded from below by zero, independently of the metro area's minority share. We define the *between-jurisdiction segregation index* as

$$\bar{\eta}^2 = \frac{\bar{\theta} - m}{1 - m}.$$

For the New York metropolitan area, between-district Black isolation is 25% ($\bar{\theta} = 0.25$), which is lower than total isolation across blocks (49%), but higher than the Black population share in the metropolitan area as a whole (16%). The resulting between-district segregation index is $\bar{\eta}^2 = 0.11$, reflecting that segregation of Black households across jurisdictions is relatively low relative to

8

total segregation. Specifically, the ratio of between-segregation to total segregation $\bar{\eta}^2/\eta^2$ is 0.28, indicating that about a quarter of segregation in the New York metro area takes place between jurisdictions as opposed to within jurisdictions.

2.4 Decomposing Metropolitan Segregation

Using between-segregation, we can decompose total metropolitan segregation into between- and within-jurisdiction components. Total segregation can be written as between-jurisdiction segregation plus a weighted mean of within-jurisdiction segregation across all the jurisdictions in the area:

$$\eta^2 = \bar{\eta}^2 + \sum_{j=1}^{J} \lambda_j \eta_j^2$$

with

$$\lambda_j = \frac{m_j (1 - m_j) n_j}{m (1 - m)},$$

where $n_j = N_j/N$ is the share of the MA-wide population living in j. We call the term $\sum_{j=1}^{J} \lambda_j \eta_j^2$ *within-jurisdiction segregation*, capturing a weighted mean of neighborhood segregation within jurisdictions. Larger population jurisdictions, and those with a minority share closer to 50% receive more weight in this average.

Figure 5 explains the intuition of the decomposition, using simulated a dataset. The square denotes a metropolitan area consisting of two jurisdictions (left and right), with each scatter dot corresponding to a neighborhood (census block). The heat coloring denotes the share of neighborhoods' population that is from the minority group. In the first panel, all of the area's segregation is due to within-jurisdiction segregation, since the minority population share of both jurisdictions is similar. In the middle panel, all the segregation in the area is due to between-jurisdiction stratification; within each jurisdiction there is no variation in neighborhood demographic, but the left jurisdiction has a much lower minority share than the right one. In the rightmost panel, both between- and within-jurisdiction are at play; there is some imbalance in the racial composition of neighborhoods within jurisdictions, and there is a large gap in the minority population share across the two jurisdictions.

We can use this intuition to understand the national decomposition statistics of metropolitan segregation over the period 1990-2020, shown in Figure A.3. Mean Black segregation has been in steady decline since 1990, when it was about 0.48, to less than 0.30 in 2020. The different colors in the bar graph show the decomposition. In 1990, between-district segregation drove about a fourth of Black-White segregation. It is apparent that the large decrease in segregation is due to increased Black-White exposure within school districts, and to a much lesser extent to reductions

9

in segregation between districts. In 2020, between-district segregation explained a third of average Black metropolitan stratification. On the other hand, the segregation of both the Hispanic and Asian populations, while considerably lower than that of Black residents, has increased during the period 1990-2020. Total segregation for Hispanic households peaked in 2010, decreasing slightly in 2020. Asian segregation, while still the lowest of the three, is increasing at a fast rate, both due to within and between-jurisdiction stratification.

The statistics above provide a useful summary of national segregation patterns, but they mask rich heterogeneity in the role of between-jurisdiction stratification across metropolitan areas. The scatter plots in Figure 7 explore this by plotting between-district segregation against within-district segregation of metropolitan areas. The diagonal lines are "iso-segregation" lines, corresponding to equal levels of total segregation. It is evident that metro areas differ substantially in the decomposition. For instance, both Detroit and Chicago have similar levels of total segregation, but Detroit's segregation is driven largely by between-district stratification, whereas Chicago's is mostly due to witthin-district segregation across neighborhoods. Moreover, Figure A.7 shows the time trajectory of a selected sample of metro areas in the iso-segregation plots. Detroit has substantially decreased its segregation, largely due to big gains in between-district integration during the period 2000-2020. The Washington D.C. area shows similar patterns.

2.4.1 Extending to Administrative Boundaries

As mentioned above, most local governments draw administrative boundaries with important implications for public good provision. For the case of public schooling, we can further decompose segregation within school districts into a component reflecting within-district segregation between school attendance boundaries (SABs) and a component reflecting block segregation within SABs. To this end, let $k = 1, ..., K_j$ index SAZs within school district j, which are composed of blocks $i = 1, ..., I_k$. We can decompose metropolitan segregation into three parts:

$$\eta^2 = \bar{\eta}^2 + \sum_{j=1}^{J} \lambda_j \eta_j^2$$

$$= \underbrace{\bar{\eta}^2}_{\text{Between-district}} + \underbrace{\sum_{j=1}^{J} \lambda_j \bar{\eta}_j^2}_{\text{Between-SAB}} + \underbrace{\sum_{j=1}^{J} \lambda_j \sum_{k=1}^{K_j} \lambda_{kj} \eta_{kj}^2}_{\text{Within-SAB}},$$

where $\bar{\eta}_j$ measures the between-SAB segregation in district j, and η_{kj}^2 is the within-SAB segregation in SAB k of district j.

In Figure 6, we show this decomposition for average metropolitan segregation across the four

major US Census regions. For Black residents, segregation is highest in the Midwest, about 0.41. Nearly half of the total segregation of Midwest cities is due to stratification across school district boundaries, and only a small share can be attributed to stratification across SAZs within school districts. These results contrast with the South and the Northeast, where the role of between catchment zone segregation within districts is larger – in the Northeast, driving a third of total metro segregation – and between-district segregation contributes slightly less, although still an important driver of observed stratification patterns. In the West, Black residential segregation is much lower, but relatively high for Hispanic residents. Slightly less than a third of Hispanic segregation in the West is due to between-district sorting, and about a quarter is due to within-district sorting across SABs.

3   Demographic Discontinuities at Local Government Boundaries

Our descriptive analysis has thus far established that jurisdictional segregation drives an important share of total stratification patterns in US metropolitan areas. However, these statistics do not grapple directly with the spatial structure of neighborhoods and the amenities near local government boundaries. It is possible that segregation between jurisdictions is entirely driven by the division of metropolitan areas into clusters of neighborhoods with similar amenity levels. In such a case, household sorting may be entirely due to neighborhood sorting, and only spuriously correlated with local governments and their boundaries. In contrast, jurisdictional segregation could be exclusively driven by sorting across local government boundaries, in which case boundaries and access to public goods would play a central role in explaining patterns of segregation.

3.1   A Model of Household Sorting Across Space

To make these ideas precise, we now develop a residential sorting model near a local government boundary with smoothly varying neighborhood amenities but a discontinuous change in the quality of public goods as we cross from one side of the boundary to the other.[3] A unit mass of households is divided into two types $t \in \{M, W\}$: minorities and whites, of which minorities make up a fraction m. Each type of household draws income $y \in [\underline{y}, \overline{y}]$ from a separate distribution $F_t(y)$, as illustrated in Panel A of Figure 9.

Households sort across locations on the unit interval $\ell \in [0, 1]$, with continuous and strictly increasing neighborhood amenities $a(\ell)$. A boundary at $\ell = 0.5$ divides locations into two jurisdic-

---

[3]This model adapts Bilal and Rossi-Hansberg (2021) to the boundary neighborhood setting. Public goods with spatial externalities such as air quality vary smoothly across local government boundaries as well. But many of the core functions of local government – access to schools, emergency safety provision, land-use regulation, and others – change discontinuously at boundaries.

tions $j \in \{L, R\}$: the jurisdiction to the left provides a low-quality public good x_L, and the one to the right provides a high-quality public good $x_R > x_L$.[4] Households value locations according to $v_t(\ell) = \lambda_t x_j + a(\ell)$, as shown in Panel B of Figure 9, where λ_t can be interpreted either as a preference for the public good, or equivalently as differential access to the public good, as we elaborate below. Given a price function $p(\ell)$, households then trade off the value of a residential location against private consumption c (the numeraire good):

$$
\begin{aligned}
&\max_{c,\ell} \log c + \phi v_t(\ell) \\
&\text{s.t. } c + (1 + \pi_t)p(\ell) \leq y
\end{aligned}
\tag{1}
$$

where $\pi_M \geq \pi_W = 0$ is a premium minorities may have to pay for housing, as we explain in more detail below. This household problem yields optimal consumption decisions $c_t^*(y)$ and location decisions $\ell_t^*(y)$ as a function of household type and income.

To close the model, we assume that each location has a fixed supply of one unit of housing. We can then define a *sorting equilibrium* as consumption and location decisions as well as a price function such that (a) households behave optimally in (1), and (b) the housing market clears in every location $\ell \in [0, 1]$:

$$
m \int_{\underline{y}}^{\overline{y}} 1\left[\ell_M^*(y) \leq \ell\right] dF_M(y) + (1 - m) \int_{\underline{y}}^{\overline{y}} 1\left[\ell_W^*(y) \leq \ell\right] dF_W(y) = \ell
$$

where the left-hand side is the share of households that demands housing in locations up to ℓ, and the right-hand side is the share of housing supplied in these locations. The budget set constraining a household's consumption-location tradeoff in equilibrium takes on whatever shape is necessary to evenly allocate households across all locations, as illustrated in Panel C of Figure 9: Points (a) and (b) are optimal decisions for households with the same valuation for public goods but with different incomes, whereas points (a) and (c) have different preferences but the same income. Hence, the equilibrium price function that clears all local housing markets may be discontinuous at the boundary and convex in the location index.

Model predictions. This model predicts that there can only be a discontinuity in the minority share at the boundary as illustrated in Panel D of Figure 9 if at least one of two conditions holds:

---

[4]For simplicity, we treat the quality of the public good as exogenous to the sorting problem. This is consistent with the case in which the unit interval of locations only makes up a small share of neighborhoods of the two jurisdictions, as is the case in our empirical application. However, if public goods were endogenously determined by the sorting behavior (through the resulting equilibrium house prices and corresponding property taxes), this would simply exacerbate the sorting dynamics illustrated here. Similarly, strategic complementarities in public goods consumption may explain why the levels of public goods differ on either side of the boundary without changing the general assessment of the driving forces underlying a discontinuity in minority shares at the boundary.

12

Either minority households benefit less from public goods, due to lower valuation or restricted access: $\lambda_M < \lambda_W$; or there is some form of price discrimination against minority households: $\pi_M > 0$.[5] As discussed above, in the standard sorting framework, preference heterogeneity is often the only channel through which household sorting by race takes place. But alternatively, minority households may not receive the same service quality or level than white households. For example, minority households may expect the quality of police services to be lower (Ang et al., 2021), or they may receive less city services than mostly white, affluent neighborhoods (Feigenbaum and Hall, 2015). Minorities may also face price discrimination through restricted access to mortgages (Hanson et al., 2016), racial assessment gaps (Avenancio-León and Howard, 2019), or other forms of housing discrimination (Christensen and Timmins, 2021; Christensen et al., 2021).

In contrast, three explanations commonly believed to be driving segregation across local government boundaries are not borne out in the context of this model. First, neighborhood amenities vary smoothly across space, unless they are interrupted by a barrier such as a highway. While these types of barriers are common, we show that discontinuities also exist in places without such barriers. Second, different income distributions between minorities and white households do *not* generate a discontinuity at the boundary. In this model, households sort perfectly by income such that the mass of households with median income (across both groups) locates exactly at the median location, that is, at the boundary. But there is no reason to believe that the minority share in the income distribution would fall discontinuously exactly at the median, and hence there cannot be a discontinuity at the boundary. Finally, strategic complementarities in amenities – valuing living near other households of a certain type – would again be smooth in space, just like other neighborhood amenities.

3.2   Estimating Boundary Discontinuities

We build additional intuition for our empirical examination of boundary discontinuities in the simulations shown in Figure 8. The left and right panels at the top represent two metropolitan areas (composed of two districts) with the same degree of between-district segregation. The plots below show scatter plots of block minority population shares against distance to the jurisdictional boundary. They show the fit the following regression specification:

$$m_{ij} = \alpha + \beta D_{ij} + f(d_{ij}) + \epsilon_{ij}$$

where $D_{ij} = 1(d_{ij} > 0)$ and d_{ij} measures the perpendicular distance between the centroid of census block i and the nearest boundary line of jurisdiction j. Negative values of d_{ij} denote the side of a

---

[5]A proof of predictions is in Appendix C

pair of jurisdictions with with fewer minority residents. The model controls for a flexible function of distance to the boundary $f(d_{ij})$, in this case a separate quadratic on each side.

For the left simulation in Figure 8, the data generating process (DGP) for neighborhood composition is determined by a linear function with a discontinuous jump at the district boundary. In the right simulation, the DGP is a continuous linear function of distance to the jurisdictional boundary. These two scenarios tell clearly different stories about the drivers of segregation, even though they have the same level of total and between-district segregation. On the left, segregation is caused by the jurisdictional boundary dividing the metropolitan area; on the right, segregation is a smooth function of geography, perhaps due to a desirable amenity located in the rightmost edge of the metro area.

In Figure 10, we provide an analogous spatial regression discontinuity plot for the Detroit metropolitan area's 2020 census block data; specifically, the line dividing Detroit Public Schools and Grosse Pointe Park Public Schools, in the easternmost part of the metro area. The left panel shows a map of the area near the boundary between the two school districts, showing census blocks weighted by total population and with heat coloring denoting the Black share of residents. The right panel shows a regression discontinuity plot for the census blocks near this district boundary. It is evident that there is massive discontinuity in the racial composition of residents as one crosses the boundary between the two districts. It would be difficult to argue that this discontinuity could be due to factors like proximity to the lake, for example. The history of Grosse Point Michigan, makes clear that this jurisdictional line was set with the intention of separating the two racial groups, and over time this separation has been reinforced by household sorting.

3.3 Discontinuities by Race and Boundary Type

How common are cases like the boundary line between Detroit and Grosse Pointe Michigan? Using data on census blocks located near jurisdictional boundaries across all metropolitan areas in the country, we estimate average spatial regression discontinuity coefficients for Black population shares, separately by each type of jurisdiction, as shown in Figure A.9. The top left panel shows national estimates for school district boundaries using a quadratic spline functional form specification. As one travels from the side of a district boundary with fewer Black residents to the side with higher Black population, there is a significant positive gradient, suggesting that the Black share of residences is increasing as one approaches a jurisdictional division.

At the jurisdictional boundary there is a significant discontinuous jump of about 2 percentage points, after which the Black share continues to increase, albeit at a lower rate. This overall pattern is mimicked by municipal boundaries (3.5 p.p. RD coefficient), and by stacked district and municipal boundaries (5.4 p.p.). The latter focus on jurisdictional lines that correspond to

both a school district and a municipal boundary. While small relative to Grosse Pointe's massive discontinuity, these results indicate that demographic discontinuities at jurisdictional boundaries are commonplace around the country, and typically exacerbates when more than one local government division coincides with a geographic line.

In similar fashion, Figure 11 presents national RD estimates across racial and ethnic groups for the years 1990, 2000, 2010, and 2020. These estimates pool variation from city-only and district-only boundary lines, as well as lines that correspond to both district and city boundaries. The top left panel shows estimates for the Black population share of census blocks. The size the RD coefficient is remarkably stable over time (estimates shown in figure legend). On the other hand, the gradient between distance to the boundary and the Black share gets flatter over time. Given the intuition we provide above, this may indicate that the intensity of sorting based on proximity to amenities, whereas the segregation attributable to boundaries is unchanging over time. Patterns differ for Hispanic and Asian residents. Hispanic residents had stable discontinuities until 2020 when the relationship changed substantially (we are still trying to understand this). For the Asian population, mean boundary discontinuities have increased over the last three decades, almost doubling between 1990-2020.

The figures above are informative, but they pool stark levels of heterogeneity across metropolitan areas. Figure 12 shows a heat map of US metropolitan areas weighted by population, summarizing the average magnitude of jurisdictional boundary discontinuities for census block Black population shares. We do not find statistically significant average discontinuities in all metropolitan areas. Those for which we cannot reject a hypothesis of no discontinuity are shown in gray. Significant discontinuities (all of which are positive) are colored according to their magnitude, deeper shades of red correspond to larger RD jumps in the Black share of residents, and darker blue shades to smaller ones. The metropolitan areas with the largest demographic discontinuities are clustered in the Midwest, led by Detroit MI, Chicago IL, Cleveland OH, and Milwaukee WI. Jurisdictional discontinuities are also stark in some smaller Northeastern metropolitan areas, including Harrisburg PA, York PA and Atlantic City NJ. In the South, discontinuities in Black residential share are largest in Virginia Beach VA, Greensboro NC, Durham NC, and Little Rock AR.

The rich heterogeneity in Figure 12 is evidence that the interaction between jurisdictional boundaries and racial segregation varies across place. Most likely, these differences are due to heterogeneity in cities' history. Historical drivers include both the impact of migration flows and ensuing residential sorting during the era of suburbanization, as well as the political processes that created the jurisdictional geography of today's metropolitan. Disentangling the separate roles of these two factors in determining demographic discontinuities at local government boundaries is an important topic of future research.

4   Discussion

4.1   Jurisdictional segregation and racial inequality in socioeconomic outcomes

Our study has shown that segregation is in big part a product of stratification across jurisdictional divisions. One lingering question is whether jurisdictional segregation is linked to existing inequality in socioeconomic outcomes by race. Our decomposition framework is well suited to make this assessment by estimating multivariate models of the metropolitan Black-White gap in average student achievement in standardized exams, as a function of segregation.

Column 1 in Table 4 shows a negative and significant coefficient from a univariate model of the achievement gap on total metropolitan segregation, indicating that more segregated areas have greater inequality on average. Column 2 adds the share of segregation attributable to between-district sorting to the model. The coefficient on total segregation decreases almost by 50% with the inclusion of the between-district share, whose coefficient is also negative and highly significant. This suggests that much of the correlation between total segregation and inequality can be explained by jurisdictional segregation. Columns 4 and 5 add controls to these models, for which the results are similar.[6]

Furthermore, column 3 adds an indicator variable to the model measuring whether the metropolitan level mean regression discontinuity estimates are significant. Interestingly, the coefficient for this indicator is also significant, negative, and its addition lowers the magnitude of both the total segregation and between-district share coefficients, a pattern that is robust to the inclusion of controls (column 6). While only suggestive, one interpretation of these correlations is that segregation that is due to demographic discontinuities across local boundaries has an independent association with, inequality; one that partly drives the overall statistical link between total segregation and the achievement gap.

4.2   Conclusion

The findings in this paper provide new facts about the drivers of segregation in metropolitan areas, highlighting the importance of local government boundary lines. The literature indicates that segregation across boundary lines is simultaneously due to issues of boundary setting and household sorting. The theoretical literature on district mergers and city annexations suggests that boundaries are endogenous outcomes of political processes, which results in strategic locations of local government boundaries. Conversely, the canonical economics literature on household sorting typically views segregation across jurisdictions exclusively as the outcome of residential choice. The

---

[6]Covariates include the gap in average free or reduced price (FRL) lunch rates between Black and White students, population share Black, share White, and indicators for 4 major Census regions.

existing evidence simply cannot distinguish between these two sources of variation.

More research is needed to disentangle the supply (political) and demand (sorting) mechanisms that drive the racial and socioeconomic stratification of urban areas. On the ground, anecdotal evidence suggests that local leaders are aware of the geographic inequalities driven by boundaries, but fear using pushing for change, citing potential unintended consequences (such as real estate depreciation and white flight). However, we do not have a clear sense of the average causal effect of boundary changes on stratification or housing markets. Our ongoing work will try partly address this knowledge gap, by studying boundary changes in school attendance boundaries over the last ten years; municipal annexations (Schönholzer and Zhang, 2018); and school district secessions.

References

Aaronson, Daniel, Jacob Faber, Daniel Hartley, Bhashkar Mazumder, and Patrick Sharkey (2021): "The Long-Run Effects of the 1930s HOLC "Redlining" Maps on Place-Based Measures of Economic Opportunity and socioeconomic success," *Regional Science and Urban Economics*, Vol. 86, p. 103622.

Aaronson, Daniel, Daniel Hartley, and Bhashkar Mazumder (2020): "The Effects of the 1930s HOLC "Redlining" Maps," *Working Paper*.

Akbar, Prottoy A, Sijie Li, Allison Shertzer, and Randall P Walsh (2019): "Racial Segregation in Housing Markets and the Erosion of Black Wealth," Working Paper 25805, National Bureau of Economic Research.

Anderson, Michelle Wilde (2008): "Cities Inside Out: Race, Poverty, and Exclusion at the Urban Fringe," *UCLA Law Review*, Vol. 55.

Ang, Desmond, Panka Bencsik, Jesse Bruhn, and Ellora Derenoncourt (2021): "Police Violence Reduces Civilian Cooperation and Engagement with Law Enforcement," *Working Paper*.

Austin, D.Andrew (1999): "Politics vs Economics: Evidence from Municipal Annexation," *Journal of Urban Economics*, Vol. 45, pp. 501 – 532.

Avenancio-León, Carlos and Troup Howard (2019): "The Assessment Gap: Racial Inequalities in Property Taxation," *Available at SSRN 3465010*.

Baum-Snow, Nathaniel and Byron F. Lutz (2011): "School Desegregation, School Choice, and Changes in Residential Location Patterns by Race," *American Economic Review*, Vol. 101, pp. 3019–46.

Bayer, Patrick, Fernando Ferreira, and Robert McMillan (2007): "A Unified Framework for Measuring Preferences for Schools and Neighborhoods," *Journal of Political Economy*, Vol. 115, pp. 588–638.

Bayer, Patrick, Robert McMillan, and Kim S. Rueben (2004): "What Drives Racial Segregation? New Evidence using Census Microdata," *Journal of Urban Economics*, Vol. 56, pp. 514 – 535.

Bilal, Adrien and Esteban Rossi-Hansberg (2021): "Location as an Asset," *Econometrica*, Vol. 89, pp. 2459–2495.

Billings, Stephen B., David J. Deming, and Jonah Rockoff (2014): "School Segregation, Educational Attainment, and Crime: Evidence from the End of Busing in Charlotte-Mecklenburg," *The Quarterly Journal of Economics*, Vol. 129, pp. 435–476.

Black, Sandra E. (1999): "Do Better Schools Matter? Parental Valuation of Elementary Education," *The Quarterly Journal of Economics*, Vol. 114, pp. 577–599.

Boustan, Leah Platt (2010): "Was Postwar Suburbanization "White Flight"? Evidence from the Black Migration*," *The Quarterly Journal of Economics*, Vol. 125, pp. 417–443.

——— (2012): "School Desegregation and Urban Change: Evidence from City Boundaries," *American Economic Journal: Applied Economics*, Vol. 4, pp. 85–108.

——— (2013): "Local Public Goods and the Demand for High-Income Municipalities," *Journal of Urban Economics*, Vol. 76, pp. 71 – 82.

Brasington, David M. (1999): "Joint Provision of Public Goods: The Consolidation of School Districts," *Journal of Public Economics*, Vol. 73, pp. 373 – 393.

Burns, Nancy (1994): *The Formation of American Local Governments: Private Values in Public Institutions*: Oxford University Press.

Caetano, Gregorio and Hugh Macartney (2021): "What Determines School Segregation? The Crucial Role of Neighborhood Factors," *Journal of Public Economics*, Vol. 194, p. 104335.

Calabrese, Stephen M., Dennis N. Epple, and Richard E. Romano (2012): "Inefficiencies from Metropolitan Political and Fiscal Decentralization: Failures of Tiebout Competition.," *Review of Economic Studies*, Vol. 79, pp. 1081 – 1111.

Card, David and Alan B. Krueger (1992): "Does School Quality Matter? Returns to Education and the Characteristics of Public Schools in the United States," *Journal of Political Economy*, Vol. 100, pp. 1–40.

Card, David, Alexandre Mas, and Jesse Rothstein (2008): "Tipping and the Dynamics of Segregation," *The Quarterly Journal of Economics*, Vol. 123, pp. 177–218.

Card, David and Jesse Rothstein (2007): "Racial Segregation and the Black–White Test Score Gap," *Journal of Public Economics*, Vol. 91, pp. 2158 – 2184.

Christensen, Peter, Ignacio Sarmiento-Barbieri, and Christopher Timmins (2021): "Racial Discrimination and Housing Outcomes in the United States Rental Market," Working Paper 29516, National Bureau of Economic Research.

Christensen, Peter and Christopher Timmins (2021): "Sorting or Steering: The Effects of Housing Discrimination on Neighborhood Choice," Working Paper 24826, National Bureau of Economic Research.

Clotfelter, Charles T. (1999): "Public School Segregation in Metropolitan Areas," *Land Economics*, Vol. 75, pp. 487–504.

Collins, Courtney A. and Erin K. Kaplan (2017): "Capitalization of School Quality in Housing Prices: Evidence from Boundary Changes in Shelby County, Tennessee," *American Economic Review*, Vol. 107, pp. 628–32.

Cutler, David M., Edward L. Glaeser, and Jacob L. Vigdor (1999): "The Rise and Decline of the American Ghetto," *Journal of Political Economy*, Vol. 107, pp. 455–506.

Derenoncourt, Ellora (2018): "Can you Move to Opportunity? Evidence from the Great Migration," *Working Paper*.

Duncan, Otis Dudley and Beverly Duncan (1955): "A Methodological Analysis of Segregation Indexes," *American Sociological Review*, Vol. 20, pp. pp. 210–217.

Epple, Dennis, Radu Filimon, and Thomas Romer (1984): "Equilibrium Among Local Jurisdictions: Toward an Integrated Treatment of Voting and Residential Choice," *Journal of Public Economics*, Vol. 24, pp. 281 – 308.

——— (1993): "Existence of Voting and Housing Equilibrium in a System of Communities with Property Taxes," *Regional Science and Urban Economics*, Vol. 23, pp. 585 – 610.

Epple, Dennis and Glenn J. Platt (1998): "Equilibrium and Local Redistribution in an Urban Economy when Households Differ in both Preferences and Incomes," *Journal of Urban Economics*, Vol. 43, pp. 23 – 51.

Epple, Dennis and Thomas Romer (1989): "On the Flexibility of Municipal Boundaries," *Journal of Urban Economics*, Vol. 26, pp. 307 – 319.

Epple, Dennis, Thomas Romer, and Holger Sieg (2001): "Interjurisdictional Sorting and Majority Rule: An Empirical Analysis," *Econometrica*, Vol. 69, pp. pp. 1437–1465.

Epple, Dennis and Holger Sieg (1999): "Estimating Equilibrium Models of Local Jurisdictions," *Journal of Political Economy*, Vol. 107, pp. 645–681.

Epple, Dennis, Allan Zelenitz, and Michael Visscher (1978): "A Search for Testable Implications of the Tiebout Hypothesis," *Journal of Political Economy*, Vol. 86, pp. 405–425.

Feigenbaum, James J and Andrew B Hall (2015): "How High-Income Areas Receive More Service From Municipal Government: Evidence From City Administrative Data," *Working Paper*.

Ganong, Peter and Daniel Shoag (2017): "Why Has Regional Income Convergence in the U.S. Declined?" *Journal of Urban Economics*, Vol. 102, pp. 76–90.

Goldin, Claudia and Lawrence F Katz (2003): "The "Virtues" of the Past: Education in the First Hundred Years of the New Republic," Working Paper 9958, National Bureau of Economic Research.

Gordon, Nora and Brian Knight (2008): "The Effects of School District Consolidation on Educational Cost and Quality," *Public Finance Review*, Vol. 36, pp. 408–430.

——— (2009): "A Spatial Merger Estimator with an Application to School District Consolidation," *Journal of Public Economics*, Vol. 93, pp. 752 – 765.

Graham, Bryan S. (2018): "Identifying and Estimating Neighborhood Effects," *Journal of Economic Literature*, Vol. 56, pp. 450–500.

Guryan, Jonathan (2004): "Desegregation and Black Dropout Rates," *American Economic Review*, Vol. 94, pp. 919–943.

Hanson, Andrew, Zackary Hawley, Hal Martin, and Bo Liu (2016): "Discrimination in Mortgage Lending: Evidence from a Correspondence Experiment," *Journal of Urban Economics*, Vol. 92, pp. 48–65.

Hsieh, Chang-Tai and Enrico Moretti (2019): "Housing Constraints and Spatial Misallocation," *American Economic Journal: Macroeconomics*, Vol. 11, pp. 1–39.

Kenny, Lawrence W. and Amy B. Schmidt (1994): "The Decline in the Number of School Districts in the U.S.: 1950-1980," *Public Choice*, Vol. 79, pp. 1–18.

Kremer, Michael and Eric Maskin (1996): "Wage Inequality and Segregation by Skill," Working Paper 5718, National Bureau of Economic Research.

Li, Nicholas Y. (2021): "Housing Market Channels of Segregation," *Working Paper*.

Monarrez, Tomas (2021): "School Attendance Boundaries and the Segregation of Schools in the US," *Working Paper*.

Nelson, Michael A. (1990): "Decentralization of the Subnational Public Sector: An Empirical Analysis of the Determinants of Local Government Structure in Metropolitan Areas in the U. S.," *Southern Economic Journal*, Vol. 57, pp. 443–457.

Rice, Kathryn T., Leora S. Waldner, and Russell M. Smith (2014): "Why New Cities Form: An Examination into Municipal Incorporation in the United States 1950–2010," *Journal of Planning Literature*, Vol. 29, pp. 140–154.

Richards, Meredith and Kori Stroub (2014): "The Fragmentation of Metropolitan Public School Districts and the Segregation of American Schools: A Longitudinal Analysis," *Teachers College Record*, Vol. 116, pp. 1–30.

Rusk, David (1993): *Cities Without Suburbs*: Woodrow Wilson Press.

Sahn, Alexander (2021): "Racial Diversity and Exclusionary Zoning: Evidence from the Great Migration," *Working Paper*.

Schelling, Thomas C. (1971): "Dynamic Models of Segregation," *The Journal of Mathematical Sociology*, Vol. 1, pp. 143–186.

Schönholzer, David (2021): "Measuring Preferences for Local Public Goods," *Working Paper*.

Schönholzer, David and Calvin Zhang (2018): "Valuing Local Public Goods Using Municipal Annexations," *Working Paper*.

Shertzer, Allison, Tate Twinam, and Randall P. Walsh (2016): "Race, Ethnicity, and Discriminatory Zoning," *American Economic Journal: Applied Economics*, Vol. 8, pp. 217–46.

Tiebout, Charles M. (1956): "A Pure Theory of Local Expenditures," *Journal of Political Economy*, Vol. 64, pp. pp. 416–424.

Trounstine, Jessica (2018): *Segregation by Design: Local Politics and Inequality in American Cities*: Cambridge University Press.

U.S. Census Bureau Government Division (2013): *2012 Census of Governments: Individual State Descriptions*: U.S. Government Printing Office, Washington, DC.

Weiher, Gregory R (1991): *Fractured Metropolis, The: Political Fragmentation and Metropolitan Segregation*: Suny Press.

Figures

Figure 1: Spatial distribution of racial groups, New York City, 2020
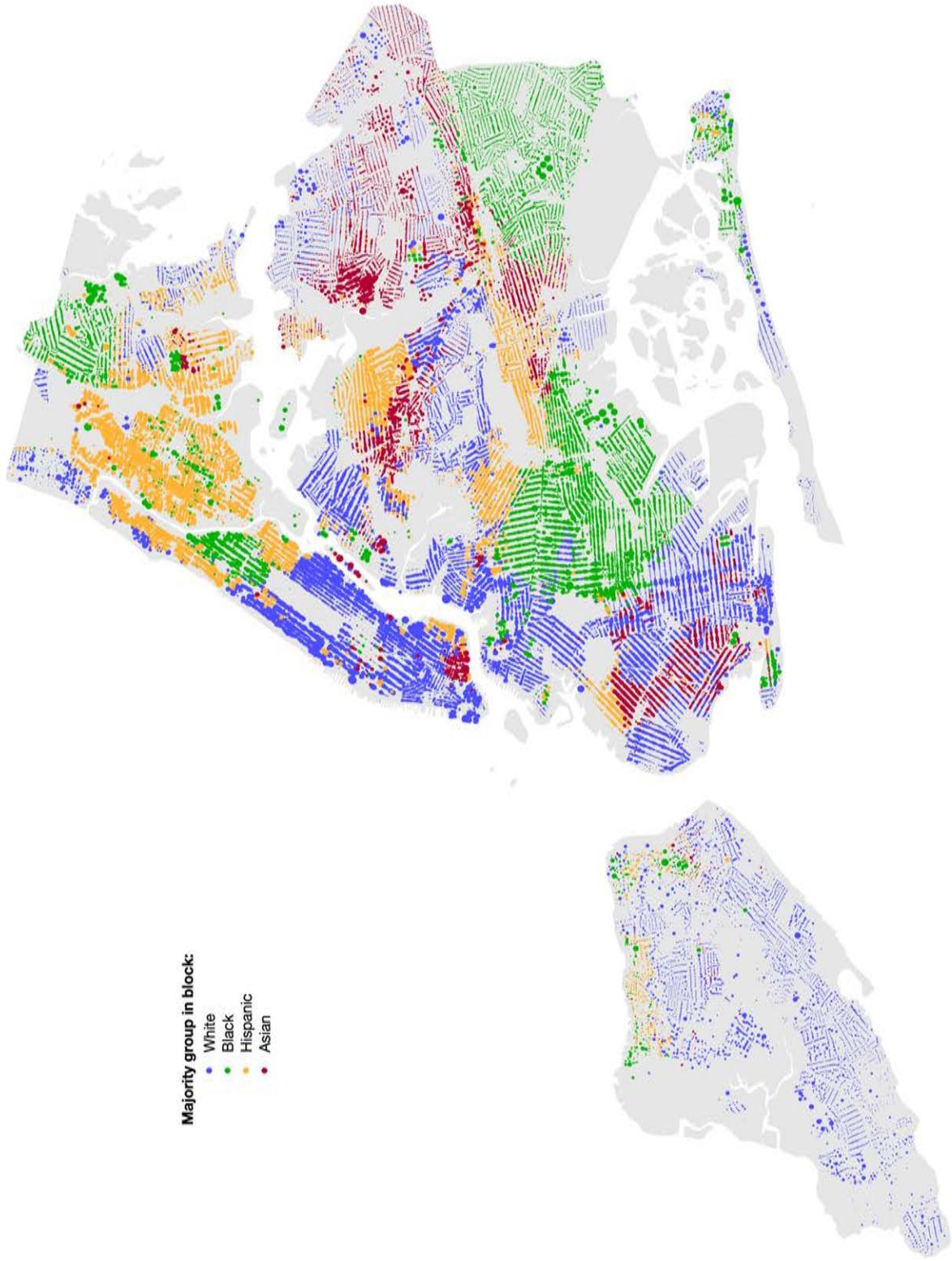
Notes: Map of the census blocks making up New York City. Population-weighted scatter dots correspond to the average latitude-longitude location of each block. Population demographic estimates based on 2020 census data. Majority population is determined using only the four racial and ethnic groups reported.

24

Figure 2: Distribution of within-jurisdiction segregation over time for districts, cities, and counties

25

Figure 3: Spatial distribution of racial groups by blocks across school districts, New York metropolitan area, 2020

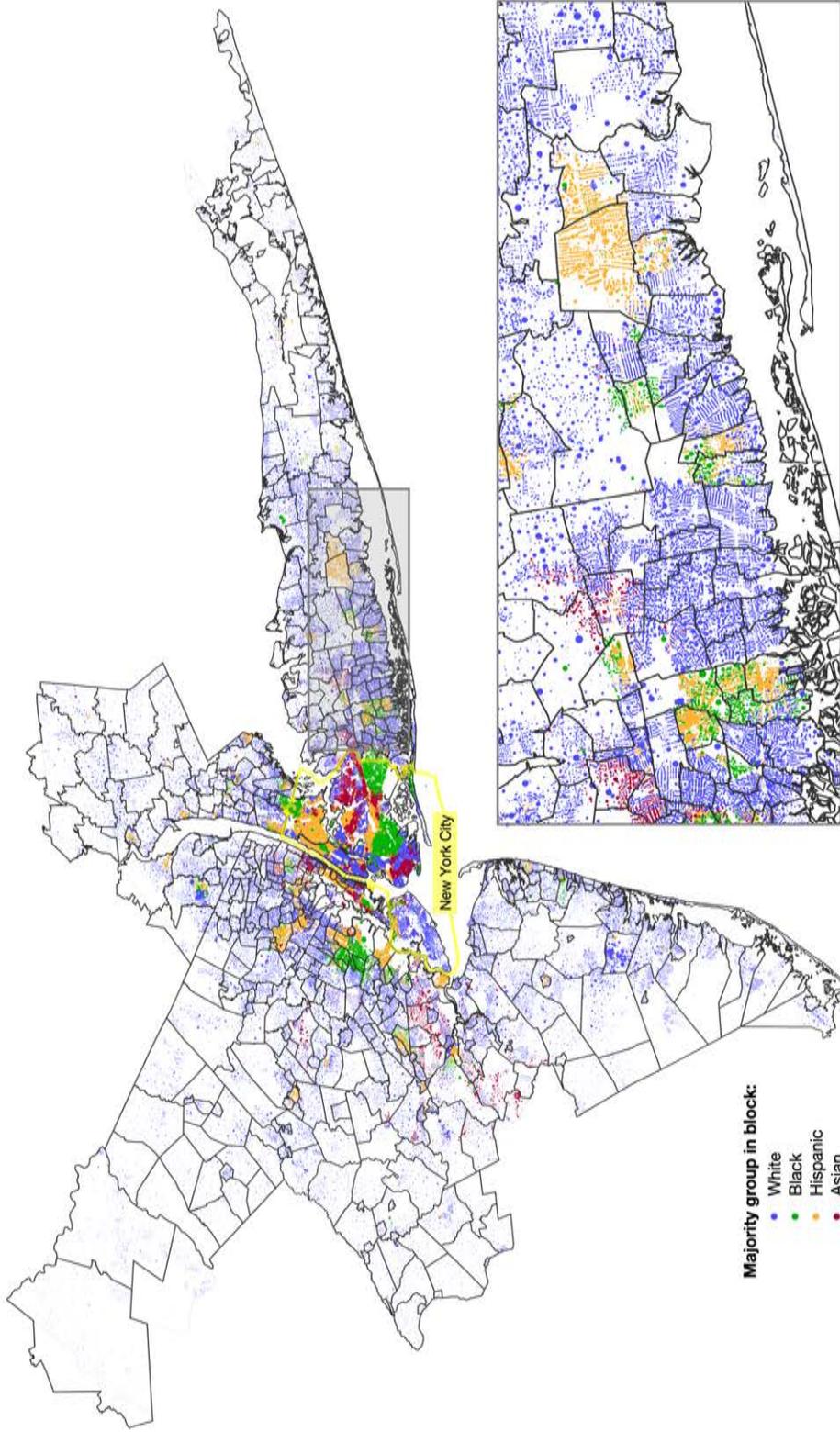Majority group in block:
- White
- Black
- Hispanic
- Asian

Notes: New York Metropolitan Statistical Area (MSA) and 502 independent school districts (local education agencies) according to 2020 census definitions. Population-weighted scatter plot shows the latitude/longitude location of census block centroids, with colors corresponding to the majority racial group of block residents. Figure shows a zoomed in section of western Long Island.

Figure 4: Segregation of Black households across metropolitan areas, 1990-2020
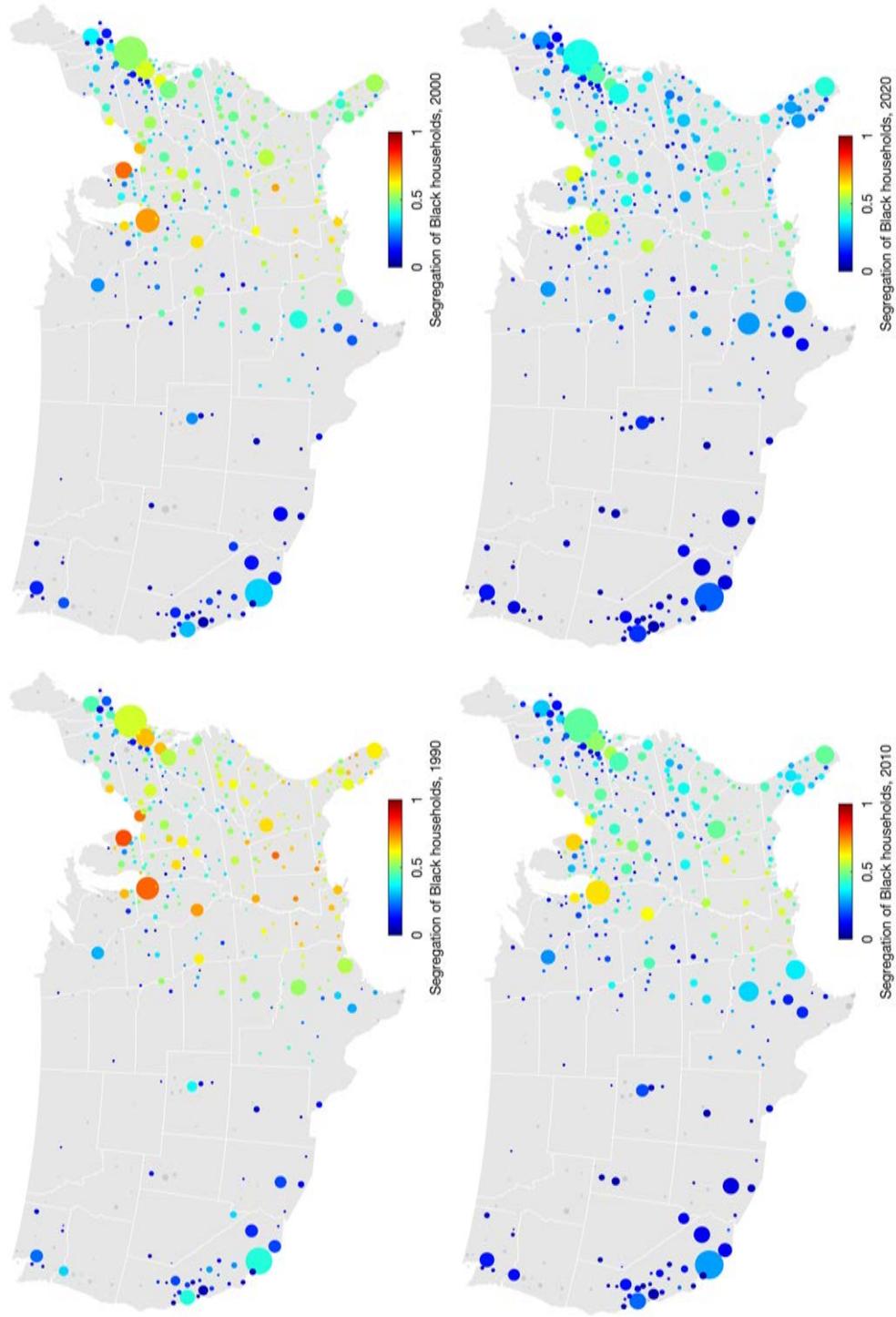
Notes: Location of US metropolitan areas, weighted by population. Heat coloring corresponds to total metropolitan segregation levels for Black residents. Estimates based on the variance ratio index, using 1990, 2000, 2010, and 2020 census block data.

Figure 5: Illustration of within-segregation and between-segregation with simulated data
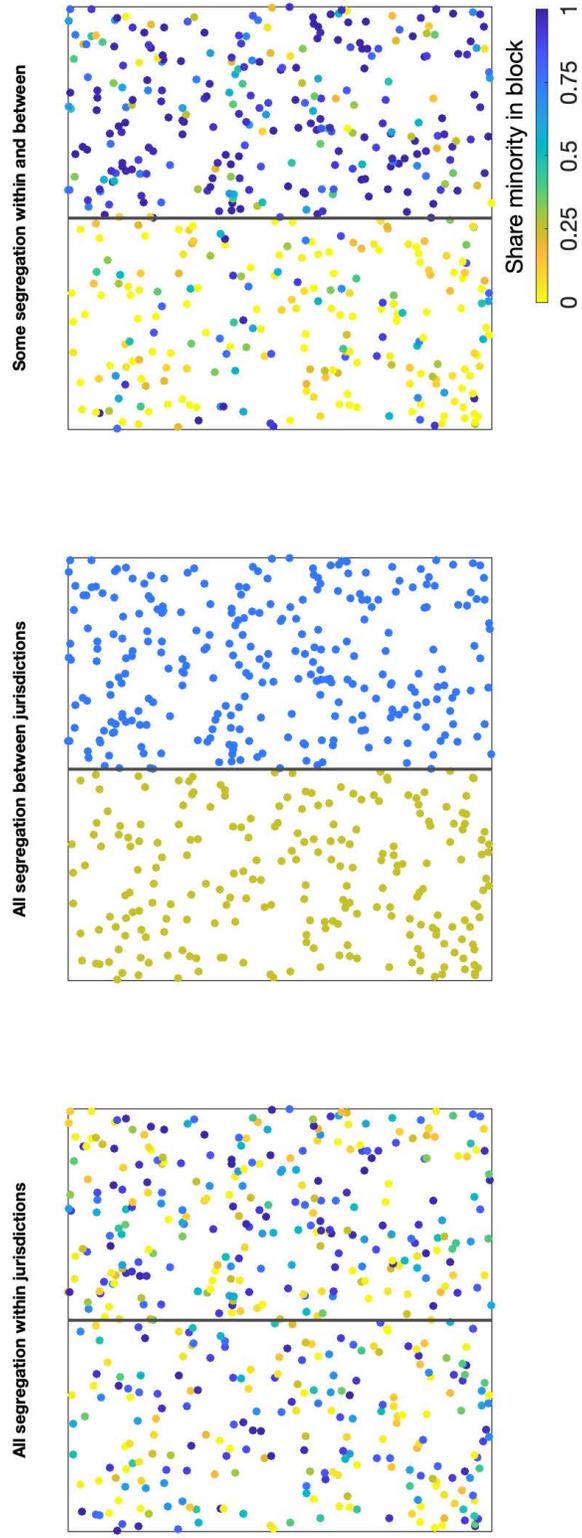
Notes: Simulated data. All three simulated MAs have the same minority share $m = 0.5$ and the same level of total segregation.

Figure 6: Decomposition of mean metropolitan segregation across US Census Regions, 2020.
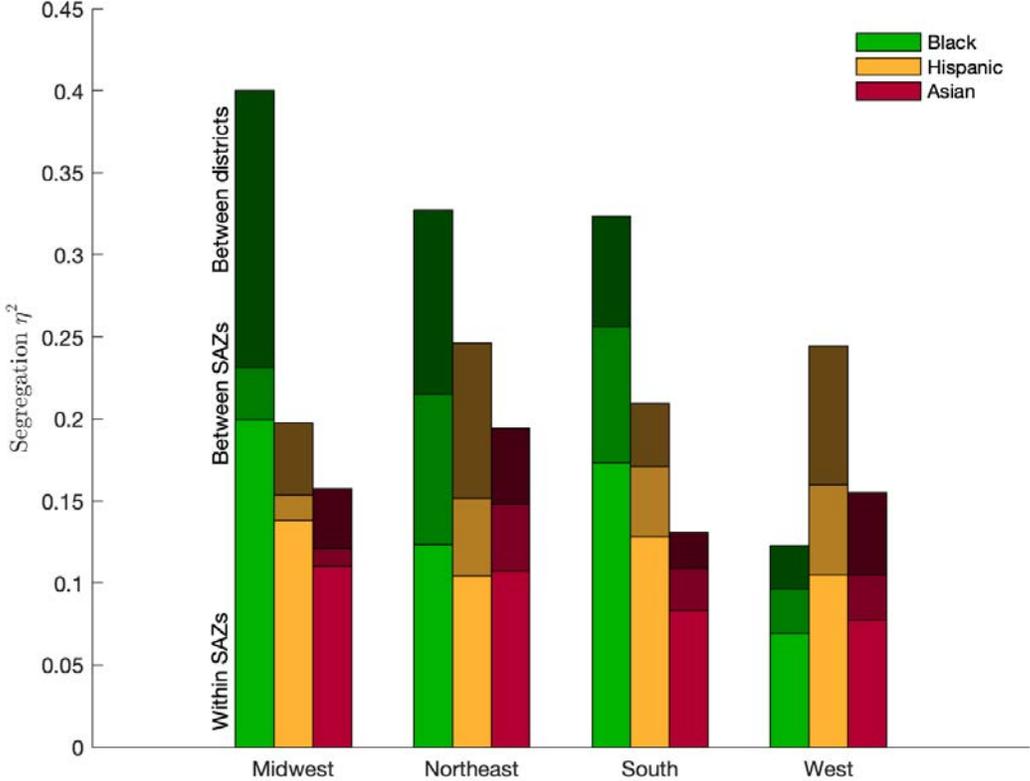
Notes: SAZ = School Attendance Zones. Average metropolitan segregation by US Census region, based on 2020 census block data. Decomposition terms shown in different color shades, according to the description in Section 4.5.1.

Figure 7: Relationship between- and within-school district segregation across metropolitan areas in 2020.
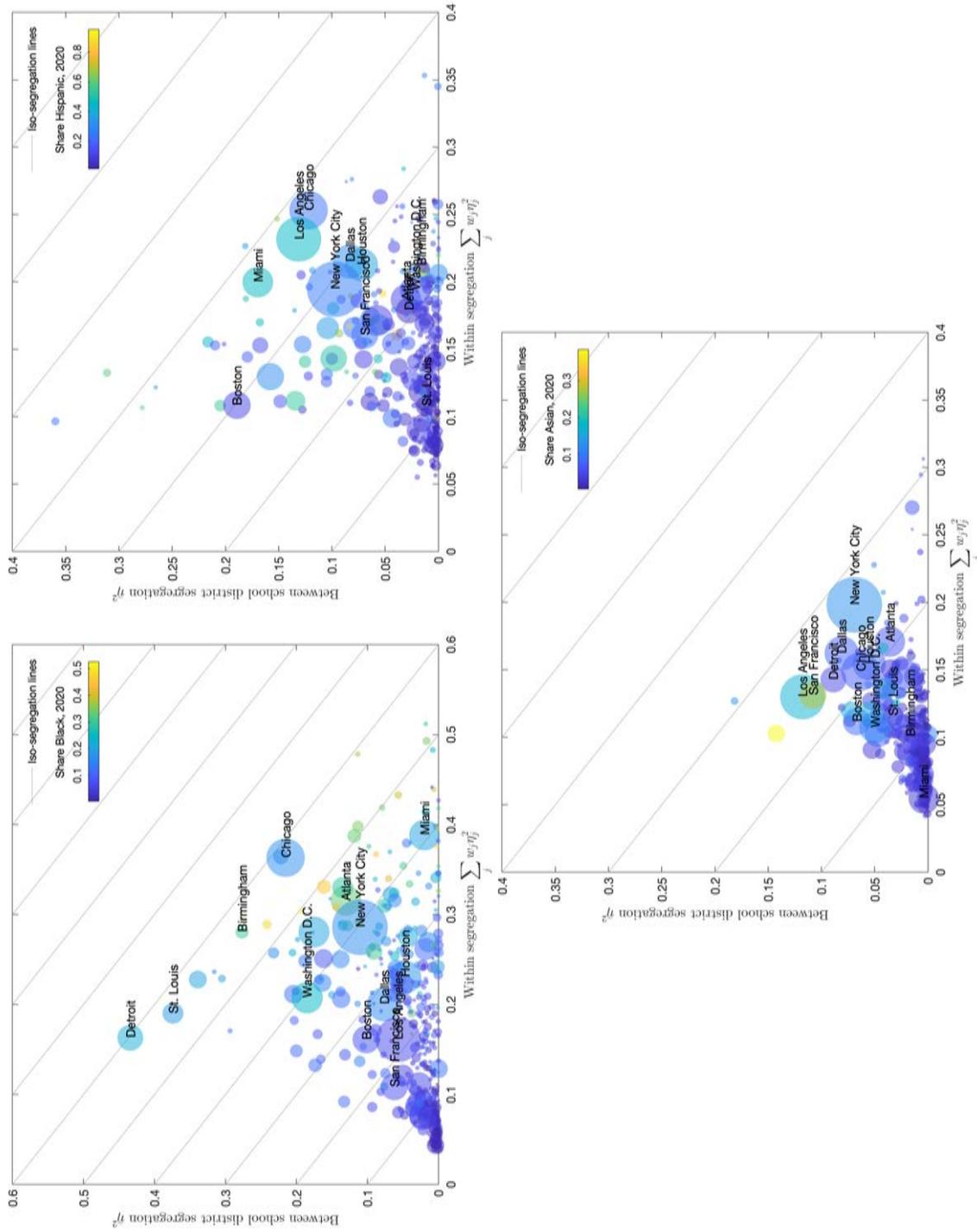
Notes: Population-weighted scatter plot of metropolitan areas, plotting between-district and within-district segregation. Heat coloring denotes the racial group's share of the population. Diagonal lines correspond to an "iso-segregation" locus of equal levels of total segregation.

Figure 8: Spatial gradient near boundary with simulated data
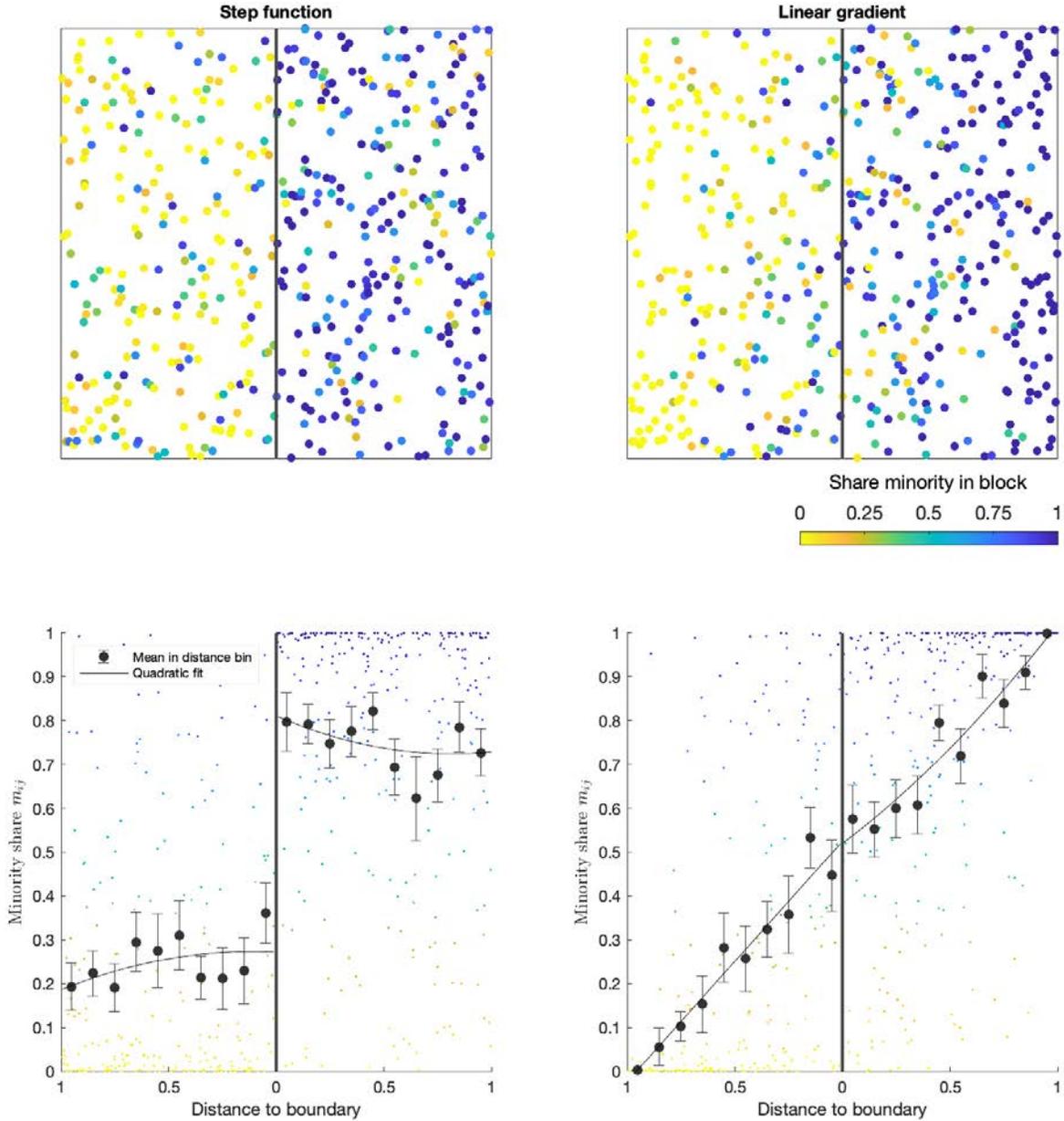
Notes: Two simulated metro areas, each with two jurisdictions. Both metro areas are generated to have the same minority share ($m = 0.5$), total segregation ($\eta^2 = 0.625$), and between-district segregation. The top panels show the hypothetical geography of these metro areas, with a heat map corresponding to blocks' (scatter dots) minority resident share. The bottom panels show spatial regression scatter plots, where the vertical axis measures the block minority share and horizontal axis measures distance to the district boundary line in kilometers. In the left panel, the data generating process (DGP) is a quadratic spline with a discontinuity at the jurisdictional boundary. In the right panel the DGP is a linear continuous function of distance to the boundary.

31

Figure 9: Illustration of spatial sorting model
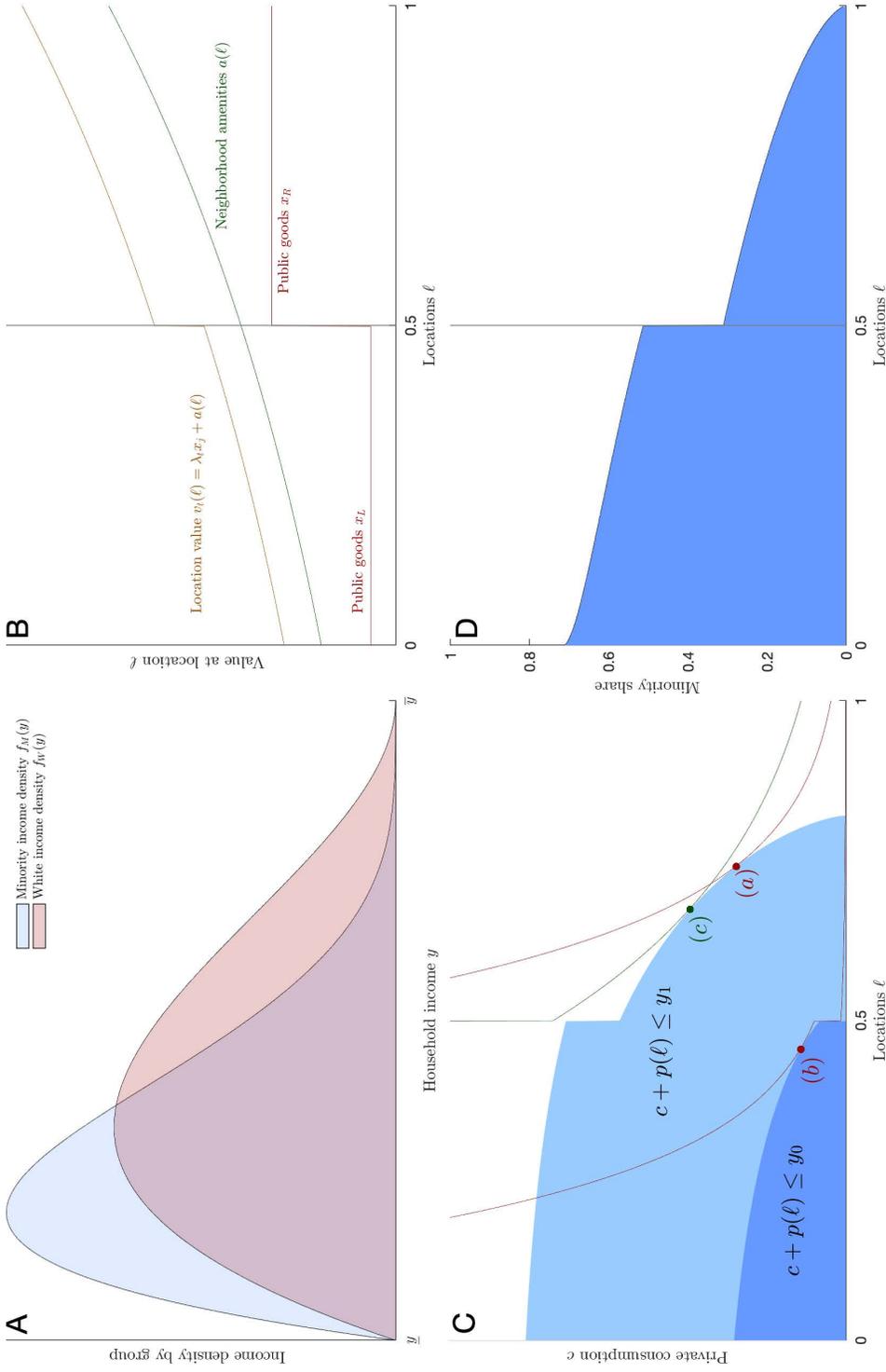
Notes: Panel A: Densities of household income by type. Panel B: Value of location $v_t(\ell)$ as a function of household type valuation of the public good λ_t, the quality of the public good x_j, and neighborhood amenities $a(\ell)$. Panel C: Equilibrium budget sets for different incomes $y_1 > y_0$ and public good valuations: high valuation in red, low in green. Panel D: distribution of minority share near boundary with discontinuity.

Figure 10: Example of boundary discontinuity in Black residential share: Detroit Public Schools and Grosse Pointe Park Public Schools, MI, 2020
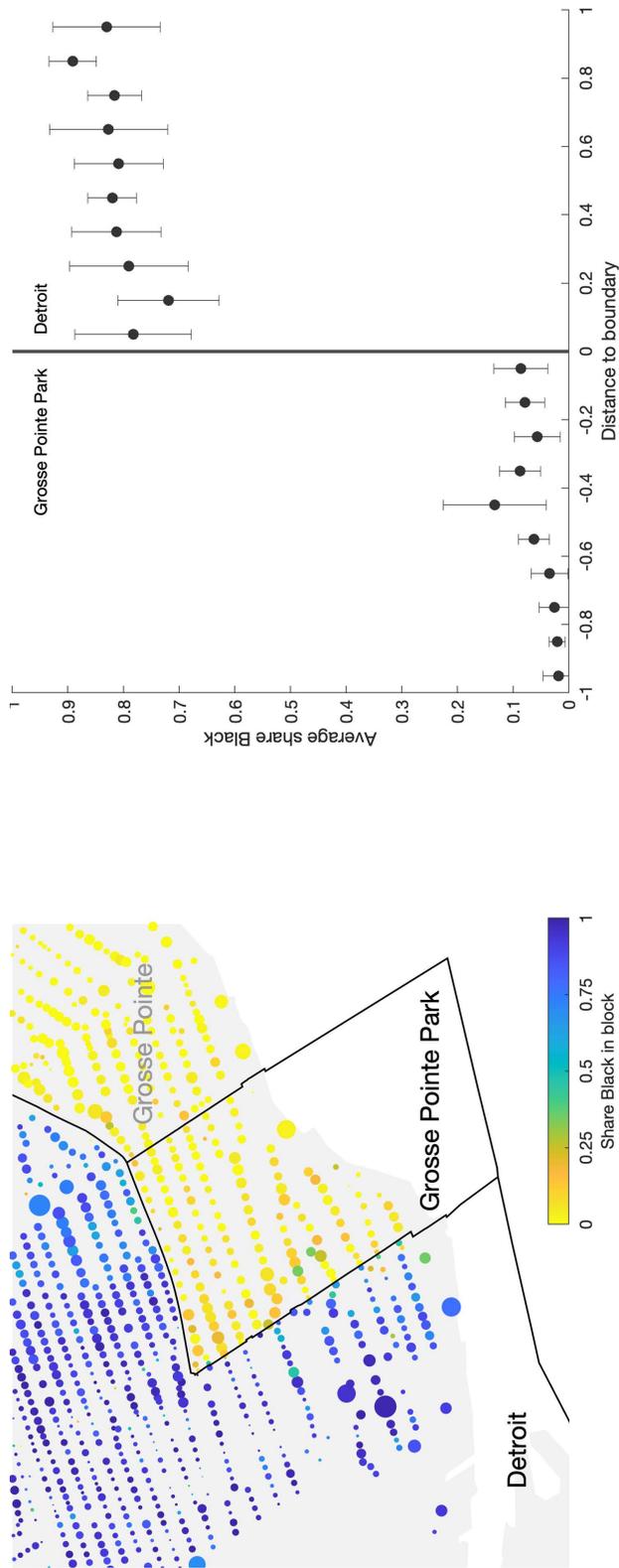
Notes: Left panel shows a map of the jurisdictional boundary between Detroit Public Schools and Grosse Pointe Park Public Schools in the Detroit, MI metropolitan area. Population-weighted latitude/longitude location of census block centroids is shown; heat coloring corresponds to the Black share of block population. Right panel shows the spatial regression discontinuity plot of blocks near (within 1 kilometer) of the district boundary. Horizontal axis measures census blocks' perpendicular centroid distance to the boundary line. Vertical axis shows the Black share of total census block population in 2020. Scatter plot shows binned means, with bins determined by equally-sized distance steps.

Figure 11: National average demographic discontinuities at jurisdictional boundaries for all years, by racial group
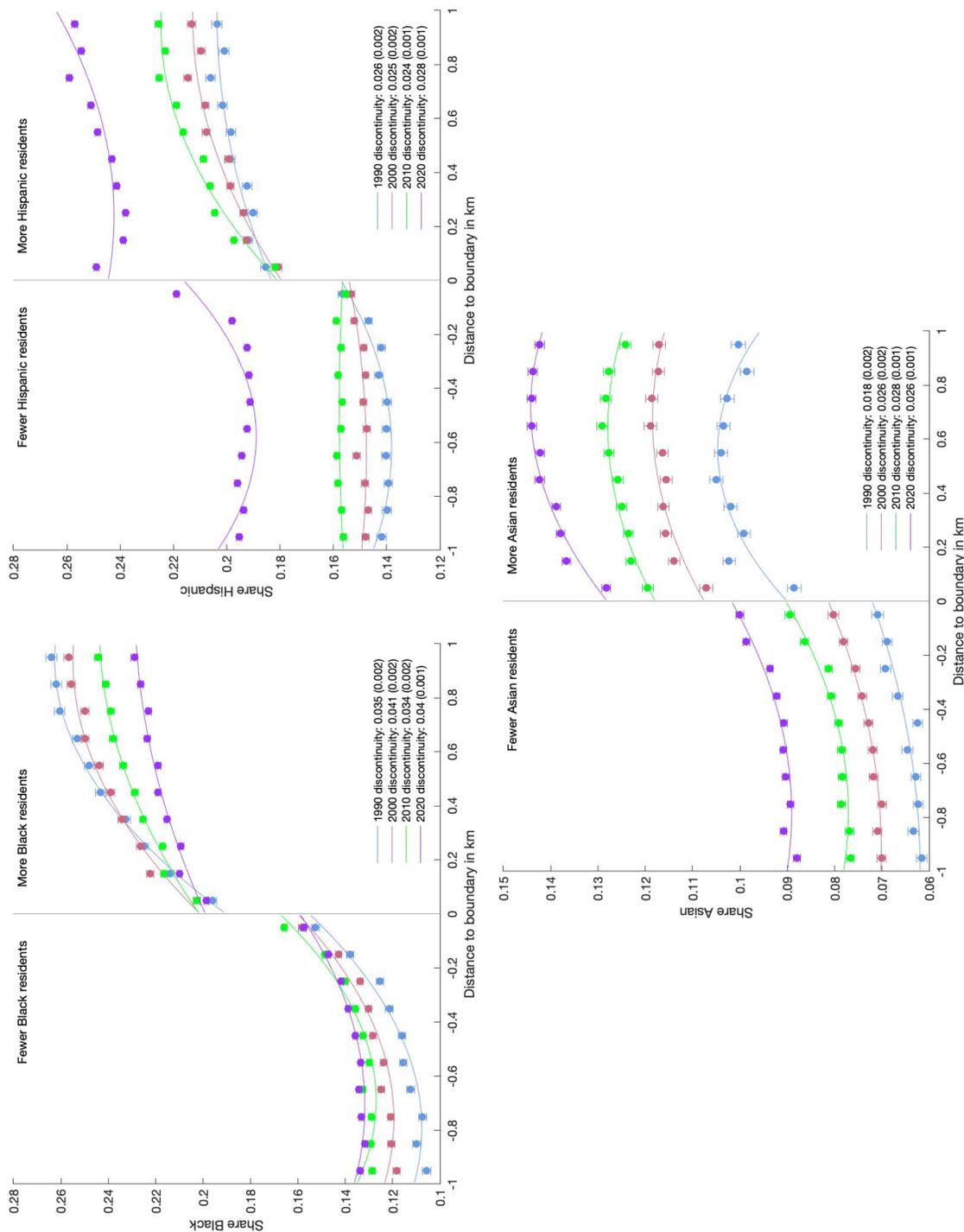
Notes: Spatial regression discontinuity (RD) plots of demographic composition against block distance to jurisdictional boundaries. Horizontal axis measures census blocks' perpendicular centroid distance to jurisdictional boundaries, where negative distance values correspond to the jurisdiction with fewer racial minority residents. Vertical axis shows the share of census block population from each racial and ethnic group, in 1990, 2000, 2010, and 2020. Scatter plot shows binned means, with bins determined by equally-sized distance steps. Estimation sample is restricted to census blocks within 1 kilometer of a jurisdictional boundary and boundaries with at least one side with 5% racial minority residents or more, resulting in about 1.5M census blocks across 15,000 boundaries. RD coefficient (along with robust standard error) and quadratic spline fit reported.

34

Figure 12: Average spatial RD coefficient for Black population share at jurisdictional boundaries, across metropolitan areas, 2020

Average boundary discontinuity in share Black households
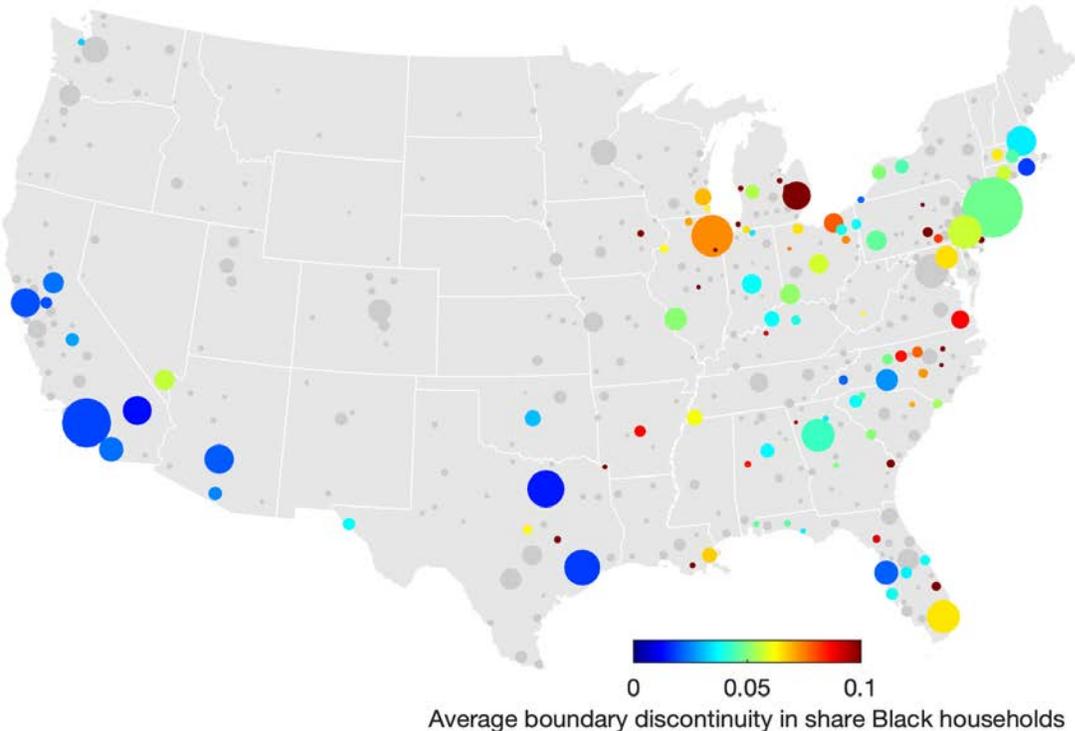
Notes: Map of US metropolitan areas weighted by total population. Colors denote the magnitude of a metropolitan area-specific RD coefficient of block population share Black as a function of block perpendicular distance to local government boundaries (municipal and school district). Grayed out metropolitan areas do not have a statistically significant spatial RD coefficient at the 5% confidence level.

Tables

Table 1: Segregation within cities, school districts, and counties in 2020

	Cities			School districts			Counties		
	P(10)	P(50)	P(90)	P(10)	P(50)	P(90)	P(10)	P(50)	P(90)
Panel A: Black residents									
Population share m_j	0.002	0.02	0.257	0.003	0.018	0.178	0.006	0.059	0.297
Isolation θ_j	0.05	0.136	0.518	0.059	0.128	0.423	0.089	0.243	0.602
Within-segregation η_j^2	0.038	0.1	0.311	0.045	0.101	0.29	0.073	0.186	0.427
Panel B: Hispanic residents									
Population share m_j	0.014	0.05	0.282	0.017	0.06	0.354	0.019	0.063	0.254
Isolation θ_j	0.084	0.172	0.446	0.099	0.187	0.511	0.119	0.198	0.451
Within-segregation η_j^2	0.05	0.108	0.239	0.06	0.118	0.252	0.085	0.144	0.262
Panel C: Asian residents									
Population share m_j	0	0.009	0.063	0.002	0.012	0.083	0.003	0.014	0.062
Isolation θ_j	0.045	0.094	0.226	0.061	0.107	0.246	0.074	0.111	0.22
Within-segregation η_j^2	0.035	0.073	0.17	0.047	0.083	0.181	0.06	0.095	0.178
Panel D: General statistics									
Jurisdiction population N_j	0.3	3.7	58.3	1.1	12.1	79	15.3	99.6	585.7
Number of jurisdictions	10,693	—	—	7,429	—	—	1,165	—	—

Notes: Estimates based on 2020 census block data. Population share based on total population in the jurisdiction. P(10), P(50), and P(90) refer to the 10th percentile, the median, and the 90th percentile, respectively. Isolation index defined in section 4.3. Within-jurisdiction segregation based on the variance ratio index, defined in section 4.3.

Table 2: 20 most segregated and most integrated metropolitan areas for Black households, 2020

		2020				Change 1990-2020		
	Rank	m	η^2	$\bar{\eta}^2$	$\bar{\eta}^2/\eta^2$	Δm	$\Delta\eta^2$	$\Delta\bar{\eta}^2$
Panel A: **Most segregated metro areas**								
Detroit-Warren-Dearborn, MI	1	0.219	0.597	0.434	0.727	0.993	0.748	0.727
Milwaukee-Waukesha, WI	2	0.163	0.587	0.222	0.379	1.193	0.853	1.223
Chicago-Naperville-Elgin, IL-IN-WI	3	0.164	0.579	0.215	0.372	0.877	0.745	0.824
Cleveland-Elyria, OH	4	0.197	0.567	0.339	0.598	1.104	0.745	1.009
St. Louis, MO-IL	5	0.18	0.564	0.374	0.663	1.086	0.781	1.048
Birmingham-Hoover, AL	6	0.294	0.557	0.277	0.496	1.055	0.724	0.809
Flint, MI	7	0.197	0.534	0.305	0.571	1.012	0.724	0.972
Jackson, MS	8	0.478	0.53	0.241	0.455	1.078	0.721	1.863
Baton Rouge, LA	9	0.347	0.511	0.113	0.222	1.08	0.748	1.992
Mobile, AL	10	0.348	0.509	0.016	0.032	1.124	0.7	10
New Orleans-Metairie, LA	11	0.333	0.506	0.118	0.234	0.967	0.743	0.535
Tuscaloosa, AL	12	0.339	0.498	0.079	0.159	1.024	0.737	0.637
Memphis, TN-MS-AR	13	0.458	0.493	0.162	0.328	1.116	0.704	1.049
Shreveport-Bossier City, LA	14	0.394	0.489	0.056	0.115	1.112	0.738	1.731
Dayton-Kettering, OH	15	0.157	0.489	0.232	0.474	1.12	0.73	0.943
Baltimore-Columbia-Towson, MD	16	0.285	0.465	0.135	0.29	1.11	0.678	0.516
Beaumont-Port Arthur, TX	17	0.241	0.464	0.206	0.444	1.039	0.678	1.087
Philadelphia-Camden-Wilmington, PA-NJ-DE-MD	18	0.204	0.456	0.175	0.384	1.11	0.666	0.907
Montgomery, AL	19	0.433	0.452	0.144	0.319	1.158	0.673	2.326
Atlanta-Sandy Springs-Alpharetta, GA	20	0.336	0.446	0.13	0.292	1.339	0.68	0.583
Median of most segregated MAs	10.5	0.29	0.508	0.19	0.375	1.095	0.727	0.99
Panel B: **Most integrated metro areas**								
Colorado Springs, CO	140	0.058	0.082	0.022	0.263	0.863	0.657	0.61
Riverside-San Bernardino-Ontario, CA	139	0.074	0.097	0.022	0.225	1.135	0.604	0.577
Phoenix-Mesa-Chandler, AZ	138	0.058	0.099	0.022	0.222	1.756	0.518	0.404
Stockton, CA	137	0.077	0.107	0.009	0.086	1.501	0.579	0.341
Reading, PA	136	0.051	0.109	0.028	0.252	1.873	0.576	0.637
Austin-Round Rock-Georgetown, TX	135	0.07	0.116	0.021	0.183	0.774	0.351	0.953
Vallejo, CA	134	0.137	0.117	0.026	0.224	1.064	0.702	0.623
Providence-Warwick, RI-MA	133	0.052	0.119	0.036	0.3	1.906	0.565	0.73
Bakersfield, CA	132	0.055	0.121	0.025	0.205	1.039	0.458	0.795
Sacramento-Roseville-Folsom, CA	131	0.07	0.121	0.033	0.272	1.05	0.632	0.565
San Antonio-New Braunfels, TX	130	0.071	0.122	0.029	0.241	1.162	0.412	0.878
Las Vegas-Henderson-Paradise, NV	129	0.127	0.129	0	0	1.363	0.381	2.077
Norwich-New London, CT	128	0.06	0.134	0.052	0.388	1.312	0.895	1.113
Worcester, MA-CT	127	0.052	0.137	0.057	0.414	2.887	1.334	2.683
Allentown-Bethlehem-Easton, PA-NJ	126	0.063	0.138	0.033	0.238	3.47	0.966	1.842
Seattle-Tacoma-Bellevue, WA	125	0.061	0.138	0.027	0.197	1.305	0.601	0.636
Naples-Marco Island, FL	124	0.062	0.17	0	0	1.636	0.416	10
San Francisco-Oakland-Berkeley, CA	123	0.071	0.17	0.062	0.363	0.629	0.417	0.387
Denver-Aurora-Lakewood, CO	122	0.056	0.171	0.05	0.291	1.01	0.457	0.854
Crestview-Fort Walton Beach-Destin, FL	121	0.08	0.172	0.006	0.036	0.934	0.517	7.679
Median of most integrated MAs	130.5	0.063	0.122	0.027	0.231	1.234	0.57	0.762

Notes: Rank: Most segregated metropolitan areas among 140 large metropolitan areas with at least 5% Black share of total population. Changes between 1990-2020 denoted by $\Delta x = x_{2020}/x_{1990}$. Values of 10 and -10 indicate more than ten-fold increases and decreases, respectively.

Table 3: Average segregation in US Metropolitan Statistical Areas

	Black				Hispanic				Asian			
	1990	2000	2010	2020	1990	2000	2010	2020	1990	2000	2010	2020
Population share	0.125	0.129	0.13	0.132	0.101	0.139	0.179	0.203	0.03	0.041	0.053	0.068
Isolation	0.523	0.462	0.412	0.373	0.275	0.336	0.372	0.373	0.136	0.159	0.187	0.209
Segregation	0.47	0.398	0.338	0.289	0.207	0.242	0.247	0.223	0.111	0.125	0.144	0.153
Panel A: County segregation												
Between counties	0.049	0.049	0.044	0.038	0.017	0.02	0.021	0.02	0.005	0.007	0.01	0.013
Within counties	0.421	0.348	0.294	0.251	0.19	0.222	0.227	0.203	0.107	0.118	0.134	0.14
Panel B: City segregation												
Between cities	0.12	0.116	0.102	0.089	0.045	0.057	0.059	0.057	0.012	0.019	0.025	0.032
Within cities	0.35	0.282	0.235	0.199	0.162	0.186	0.188	0.165	0.099	0.107	0.119	0.121
Panel C: School district segregation												
Between school districts	0.117	0.112	0.097	0.084	0.047	0.059	0.063	0.062	0.013	0.02	0.027	0.036
Within school districts	0.353	0.286	0.24	0.204	0.161	0.183	0.185	0.161	0.099	0.105	0.117	0.117
Between SAZs	—	—	—	0.061	—	—	—	0.042	—	—	—	0.026
Within SAZs	—	—	—	0.138	—	—	—	0.124	—	—	—	0.095

Notes: Estimates based on census block data. Isolation is the mean share of minority group residents, conditional on being a minority. Segregation is the variance ratio index of segregation, an isolation index adjusted for the group's population share. Between-local government segregation decompositions based on the discussion in section 3.5. SAZ = School Attendance Zone. Between-SAZ segregation decomposition based on private data from Precisely for the school year 2020-21.

38

Table 4: Correlation between racial achievement gap and metropolitan segregation components

Panel A: Black achievement gap	(1)	(2)	(3)	(4)	(5)	(6)
Total segregation	-0.41***	-0.23***	-0.19***	-0.60***	-0.44***	-0.41***
	(0.05)	(0.07)	(0.07)	(0.11)	(0.09)	(0.09)
Share of seg. between districts		-0.31***	-0.29***		-0.25***	-0.23***
		(0.07)	(0.07)		(0.07)	(0.07)
1(significant spatial RD estimate)			-0.04***			-0.03***
			(0.02)			(0.01)
Covariates				X	X	X
R^2	0.31	0.44	0.48	0.53	0.60	0.61
N	379	379	379	375	375	375
Panel B: Hispanic achievement gap	(1)	(2)	(3)	(4)	(5)	(6)
Total segregation	-0.66***	-0.50***	-0.44***	-0.44***	-0.35***	-0.33***
	(0.10)	(0.14)	(0.13)	(0.13)	(0.13)	(0.13)
Share of seg. between districts		-0.12**	-0.12**		-0.06	-0.05
		(0.05)	(0.05)		(0.06)	(0.06)
1(significant spatial RD estimate)			-0.03**			-0.04**
			(0.01)			(0.01)
Covariates				X	X	X
R^2	0.34	0.36	0.38	0.50	0.50	0.53
N	379	379	379	375	375	375
Panel C: Asian achievement gap	(1)	(2)	(3)	(4)	(5)	(6)
Total segregation	0.08	-0.07	-0.12	0.29***	0.29**	0.29**
	(0.16)	(0.26)	(0.27)	(0.11)	(0.11)	(0.11)
Share of seg. between districts		0.10	0.09		0.00	0.01
		(0.10)	(0.10)		(0.05)	(0.05)
1(significant spatial RD estimate)			0.02			-0.00
			(0.02)			(0.01)
Covariates				X	X	X
R^2	0.00	0.02	0.03	0.72	0.72	0.72
N	379	379	379	375	375	375

Notes: Robust standard errors reported in parenthesis. Metropolitan area observations weighted by population. Covariates include: the gap in average free or reduced price (FRL) lunch rates between the minority group (Black, Hispanic, or Asian) and White students, population share minority, share White, and indicators for 4 major Census regions (omitting the South).

Online Appendix

A Data

We combine Geographic Information Systems (GIS) data on local government boundaries with geographic data from four waves of the decennial census to understand segregation in the context of jurisdictional divisions. GIS data on local boundaries is obtained via the US Census Bureau's TIGER/Line data for definitions of school districts (local education agencies), cities (incorporated Census places), and counties for the decennial years 1990, 2000, 2010 and 2020. We also use a dataset on school attendance boundaries from data services firm Precisely for the school year 2019-20.[7]

Our primary definition of a neighborhood is a Census block, small geographic areas that coincide with city blocks in densely populated urban settings. Typically, researchers use census tracts as the primary unit for the analysis of segregation. However, we are interested in measuring segregation within sometimes very small units, such as small cities or school attendance boundaries, which may be composed of only one or two Census tracts. Unlike blocks, tracts may be masking important variation in neighborhood composition within these small units.[8]

We collect census block level data for the decennial censuses between 1990-2020 via the National Historical Geographic Information System (NHGIS). Our analysis focuses on population counts by race and ethnicity. We study the four largest groups by population: White, Hispanic, Black and Asian. Our segregation measures focus on the separation of the White population from the Hispanic, Black, and Asian population (see below for a measurement discussion).

Finally, we bring in data on public school inputs and outcomes, to assess the relevance of boundary divisions for existing inequality in public good provision. We collect the 2011-2017 waves of the Department of Education's Civil Rights Data Collection (CRDC), obtaining school level measures of teacher and other staff characteristics, student discipline rates, and access to advanced tracking programs. We make use of the Stanford Education Data Archive (SEDA) school level dataset on average student scores on state standardized exams over the period 2008-2017. We also exploit Georgetown University's National Education Resource Database on Schools (NERDS) school level dataset for the 2018-19 school year on total expenditures.

---

[7]We are forced to rely on privately supplied data on attendance boundaries, as the federal government does not have a regular collection of these policies.

[8]Importantly, our measures of between-jurisdiction segregation is invariant to how we define neighborhoods.

B The History of Local Government Boundaries

The US system of local governments is vast, made up of thousands of fiscally independent entities, almost all of which have the power to levy property taxes. Below the federal government and the fifty state governments, most public sector activity can be organized in three groups: two general-purpose governments – county governments and municipal governments – and school districts.[9] One noteworthy feature of US local governments (in contrast to other countries) is the separation of school districts from municipal and county governments which control services like sanitation, housing, police and fire departments. The overlay of municipal and school boundaries creates a rich patchwork of invisible lines that have important implications for public good provision.

Boundary lines are not limited to the already numerous jurisdictional lines that divide local governments. Most municipal and school district governments draw their own administrative maps, ranging from school attendance boundaries, land use zoning codes, to police and fire districts. An overlay of every administrative and jurisdictional line in any metropolitan area shows a seemingly chaotic criss-cross of lines. It is important to understand the history, intention, and ultimate impact of these urban divisions on racial segregation and racial inequality in public good provision. For example, Shertzer et al. (2016) find that predominantly minority neighborhoods in Chicago were more likely to be zoned for noxious activities as part of industrial land use.

Local governments differ dramatically in the amount of property taxes they collect, and since much of their funding is localized, service quality differs dramatically. A vast literature documents these differences in service quality across local governments and studies their causes. We provide some examples to highlight that local governments play an important role in a household's economic success and residential choice. In a classic study, Card and Krueger (1992) show that there is considerable variation in the return to education across states, and that it is substantially higher in states with better school inputs, such as lower pupil-teacher ratio and higher relative teacher pay. Epple and Sieg (1999) estimate an equilibrium model of household preferences and local public goods, finding that households value lower crime and higher education expenditures. Boustan (2013) compares house prices on either side of city-suburb boundaries over time and estimates that households are willing to pay substantial premia to live in high-income suburbs, particularly for better school quality and lower property taxes. Schönholzer (2021) pursues a similar approach to summarize household willingness to pay for all excludable public goods provided by municipalities and school districts, finding that around 11% of housing costs are due to variation in local public

---

[9]The Census Bureau also recognizes township governments and other special districts (such as independent transportation districts like Bay Area Rapid Transit (BART) in the San Francisco Bay Area) as independent bodies in the local public sector, but obtaining data on activities and boundaries for these bodies is difficult, and hence they lie outside of the scope of this study.

goods.

Given the important role local governments play in households' residential choices, we now turn to a brief summary of the boundaries that delineate the territorial extent of local governments and the nature of change of these boundaries over time. We distinguish between public education boundaries, which include school district boundaries and school attendance boundaries, and municipal service boundaries, which include city and county boundaries. The location of local government boundaries is determined both through the creation and elimination of local governments as well as changes to boundaries of existing local governments. The rules that govern boundary changes are set by state constitutions and may hence differ substantially from one state to the next.

B.1 Public Education Boundaries

Historically, US public education has been characterized by local control by independent school districts. During the early 20th century, there were practical reasons for decentralized public education provision and funding in low-density localities, derived as well from a long tradition of community control and local taxation (Goldin and Katz, 2003). Public schools were operated by nearly 117,000 independent districts during this time. Then, starting in the 1940s an era of district consolidation began that witnessed a 92% decline in the number of districts in the country. By 1980 there were only about 15,000 districts nationally, and today the number is closer to 13,000.

District mergers. The literature documenting the observable predictors of district mergers highlights the role of income and racial heterogeneity (Nelson, 1990; Kenny and Schmidt, 1994; Brasington, 1999). Gordon and Knight (2008, 2009) consider the problem facing districts with potentially many possible neighbors to merge with, and how to properly estimate the role of characteristics in driving mergers. They find that socioeconomic characteristics are an important driver of merge likelihoods.Thus, it is likely realized merge patterns are linked to the increasing between district inequality witnessed in the last decades, as descriptive evidence has suggested (Weiher, 1991; Richards and Stroub, 2014). More research is needed to understand the extent to which district mergers may have systematically exacerbated US inequality in public good provision.

School attendance boundaries. As the number of districts has fallen, intra-district attendance boundary policies have become increasingly important in determining sorting patterns. School quality varies considerably within districts, and variation in average school test scores is correlated with residential sorting and real estate prices Black (1999); Bayer et al. (2007). There is observational evidence that some districts set attendance boundaries in ways meant to influence school integration, although most adhere to boundaries closely following neighborhood demarcation Monarrez

(2021). Desegregated attendance boundaries are more prevalent in districts under a desegregation order, in those with relatively lower racial animus, and in those facing lower commuting costs, suggesting that districts' boundary choice is a product of various trade-offs. Our ongoing work attempts to describe the rate at which school attendance boundaries change and the impact that school redistricting may have on housing markets.

District secessions. While the long-run trend in the number of school districts has flattened out, school district secessions have become increasingly common in recent years, hinting at a partial reversal from the previous trend of consolidation. Recent work has shown that district secessions in Memphis, Tennessee, led to sizable impacts on the housing market (Collins and Kaplan, 2017). However, to our knowledge, there is no systematic evidence on the impact of this recent wave of secessions on patterns of racial inequality nationwide. In ongoing work with co-authors, we are undertaking a systematic analysis of the impact of recent district secession events on student achievement outcomes and inequality.

B.2 Municipal Service Boundaries

Municipalities and counties provide a wide range of services to residents, including public safety, emergency response services, utilities, transportation infrastructure, courts, and jails. County governments are in charge of some of these services throughout the US, except in Connecticut, Rhode Island, and the District of Columbia, where counties serve simply as statistical units for census enumeration. Municipal and county governments are also responsible for zoning and land use regulation, policy tools that restrict the use and development of economic activity and housing.

Unlike counties and school districts, many parts of the US lie outside *any* incorporated city. These unincorporated areas include many impoverished and high-minority urban neighborhoods (Anderson, 2008) that receive only limited urban services from their county. For example, in Los Angeles County alone, more than one million households live in such areas and are effectively excluded from urban services provided by nearby cities. But unincorporated areas are also commonly found in rural areas with little need or desire for urban services.

Incorporations. As unincorporated areas experience more development, they may choose to incorporate as a city so as to provide additional public goods and gain local control. There is a long tradition of municipal incorporation in the US, with more than ten thousand incorporations before 1900, many of them having no more than a few hundred residents. Over the course of the 20th century, the trend in the number of municipal governments has been moving in the opposite direction of that of school districts: it nearly doubled from 10,602 in 1900 to just above 19,000 in

1982. Since then, growth has leveled off, arriving at 19,495 in 2017. Incorporations are driven by a variety of local interests (Rice et al., 2014). Besides the provision of public services, residents may seek to control land use and growth. In the postwar boom of suburban cities, race and class divisions played a central role in incorporation (Burns 1994). Communities may also incorporate to fight off other cities from encroaching on their territory.

Annexations. Incorporations are not the only way that unincorporated areas may become subject to municipal governance. Another common alternative are municipal annexations – territorial expansions of existing city governments into unincorporated areas. While it is true that boundary changes between existing cities are rare (Epple and Romer, 1989), annexations of unincorporated territory are extremely common: in the last twenty years, more than 100,000 annexations occurred (U.S. Census Bureau Government Division, 2013). Most of these are "greenfield" annexations, providing city services to uninhabited territory for future housing development, but some of them affect built-up neighborhoods that were historically excluded from incorporation.

In the past, central cities sometimes absorbed entire neighboring cities, such as when New York City annexed the independent city of Brooklyn in 1898, which was the fourth-largest city in the US at the time. But over the course of the early 20th century, most states introduced laws that prevented such takeovers of existing cities. Austin (1999) finds that the ability to offset the effects of suburbanization and white flight continued to motivate annexations in the postwar era. As a result, central cities that were able to absorb most of their suburbs tend to be on firmer fiscal ground than those that became locked in by a belt of affluent but independent suburban cities (Rusk, 1993).

County Boundaries Counties constitute the basic division of state territory into local units, and as such, their number grew dramatically as the United States expanded westwards. However, as the last states joined the Union, the number of counties largely stagnated. Correspondingly, the number of county governments has been almost unchanged since 1942, falling only slightly from 3,050 to 3,031. Boundaries of counties have also changed only rarely in the last fifty years (U.S. Census Bureau Government Division, 2013).

C   Boundary Sorting Model

.

In this appendix, we show under what conditions the minority share of households is discontinuous at the boundary in the model outlined in Section 3.1. We assume that households value

locations $\phi > 0$ and public goods $\lambda_t > 0$, as well as that parameters and the distributions of incomes are such that in equilibrium, the following inequalities hold: $\ell_M^*(\bar{y}_M) > 0.5$ and $\ell_W^*(\bar{y}_W) < 0.5$ for

$$\bar{y}_t = \frac{(1 + \pi_t) \left[\Lambda_t p(0.5) - \lim_{\ell \to 0.5} p(\ell) \right]}{\Lambda_t - 1}$$

and $\Lambda_t = e^{\phi \lambda_t \Delta x}$. This assumption essentially restricts how strongly location choices of different household types can diverge in equilibrium.

Proposition. *(Discontinuous minority share at the boundary). Consider the model laid out in Section 3.1. Define $G_t(\ell) = \int 1\left[\ell_t^*(y) \le \ell\right] dF_t(y)$ as the share of households of type t that locate at ℓ or below, and let $g_t(\ell) = G_t'(\ell)$ be the density of households of type t at ℓ. The density of minority households falls discontinuously at the boundary:*

$$\lim_{\ell \to 0.5} g_M(\ell) > g_M(0.5)$$

if and only if at least one of two conditions holds:

1. *Preferences for or access to the public good are lower for minorities: $\lambda_M < \lambda_W$;*

2. *Minorities experience price discrimination in the housing market: $\pi_M > 0$.*

Proof. We proceed in three steps. First, we show that households sort along ℓ strictly according to their income. This allows us to focus on households at the boundary. Second, we show that the equilibrium price jumps at the boundary. Third, utility of minority households at the boundary is continuous in ℓ if and only if at least one of the conditions in the Proposition holds.

Step 1. $v_t(\ell)$ is strictly increasing for each t. Suppose $\ell_2 > \ell_1$, which implies $v_t(\ell_2) > v_t(\ell_1)$ for both t. For markets to clear, it must be that $p(\ell_2) > p(\ell_1)$, otherwise no household would choose ℓ_1. A household with income y of type t chooses ℓ_2 over ℓ_1 iff

$$v_t(\ell_2) - v_t(\ell_1) > \log\left(y - (1 + \pi_t) p(\ell_1)\right) - \log\left(y - (1 + \pi_t) p(\ell_2)\right).$$

The right-hand side is strictly decreasing in y. It follows that any richer household has the same preference. Hence, $\ell_t^*(y)$ is strictly increasing and continuous in y, sorting households within types by income.

Step 2. Given Step 1, there exists a strictly increasing and continuous inverse function $Y_t(\ell)$. It maps a location choice to an income level for a household type with the property that $\lim_{\ell \to 0.5} Y_t(\ell) = Y_t(0.5) \equiv \hat{y}_t$ for both t. Let $u_t(y, \ell) = \log(y - p(\ell)) + \phi v_t(\ell)$. The equilibrium price at the boundary adjusts so as to make households at the boundary indifferent between either side. Specifically, it

45

has to hold that

$$\lim_{\ell \to 0.5} \sum_t n_t u_t \left(\hat{y}_t, \ell \right) = \sum_t n_t u_t \left(\hat{y}_t, 0.5 \right),$$

where $n_M = 2m F_M(\hat{y}_M)$ and $n_W = 2(1-m)F_W(\hat{y}_W)$ are the shares of household types at the boundary. We can rewrite this as:

$$\sum_t n_t \log \left(\frac{\hat{y}_t - (1+\pi_t)\lim_{\ell \to 0.5} p(\ell)}{\hat{y}_t - (1+\pi_t)\, p(0.5)} \right) = \phi \Delta x \sum_t n_t \lambda_t \qquad (2)$$

with $\Delta x = x_R - x_L$. Note that the right-hand side is strictly positive, and therefore the left-hand side has to be positive as well. But this can only be true if $\lim_{\ell \to 0.5} p(\ell) < p(0.5)$, that is, the price jumps discontinuously at the boundary.

Step 3. To examine the behavior of $g_M(\ell)$ at the boundary, we look at how $u_M(\hat{y}_M, \ell)$ behaves at the boundary: if utility of minority households is continuous, then so is the density, and if utility drops discontinuously, then so does the density. For continuity, we require that $\lim_{\ell \to 0.5} u_M \left(\hat{y}_M, \ell \right) = u_M \left(\hat{y}_M, 0.5 \right)$, which we can write as

$$\log \left(\frac{\hat{y}_M - (1+\pi_t)\lim_{\ell \to 0.5} p(\ell)}{\hat{y}_M - (1+\pi_t)\, p(0.5)} \right) = \phi \lambda_M \Delta x, \qquad (3)$$

where the prices are such that (2) holds. If $\lambda_M = \lambda_W$ and $\pi_M = 0$, then the location choice depends only on income: $\ell_t^*(y) = \ell^*(y)$, and hence $\hat{y}_M = \hat{y}_W$. As a consequence of this and the assumptions on λ_t and π_t, (2) and (3) are identical and must both hold, and thus $g_M(\ell)$ (as well as $g_W(\ell)$) is continuous at the boundary.

In contrast, if either $\lambda_M < \lambda_W$ or $\pi_M > 0$, then $\ell_M^*(y) < \ell_W^*(y)$ and hence $\hat{y}_M > \hat{y}_W$. Higher $\hat{y}_M$ lowers the left-hand side of (3) compared to the left-hand side of (2), but due to the stated assumptions, by less than the drop on the right-hand side of (3) compared to the right-hand side of (2). Hence, the left-hand side of (3) is larger than its right-hand side, and hence $\lim_{\ell \to 0.5} u_M \left(\hat{y}_M, \ell \right) > u_M \left(\hat{y}_M, 0.5 \right)$, or equivalently, $\lim_{\ell \to 0.5} u_W \left(\hat{y}_W, \ell \right) < u_W \left(\hat{y}_W, 0.5 \right)$. $\qquad \square$

**Appendix Figures**

Figure A.1: Share Black residents in Census blocks, New York City, 2020
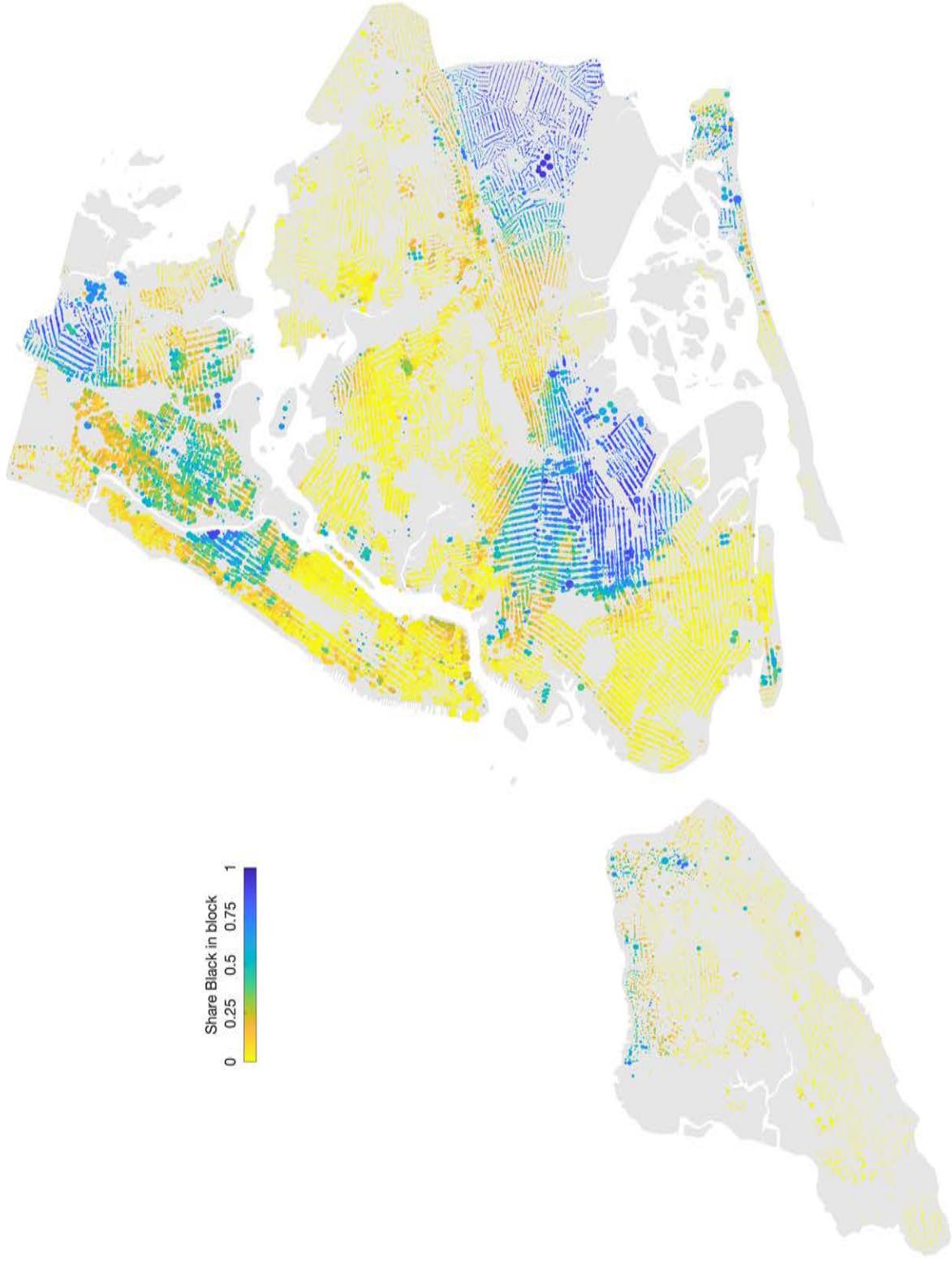
Notes: Map of the census blocks making up New York City. Population-weighted scatter dots correspond to the average latitude-longitude location of each block. Population demographic estimates based on 2020 census data. Heat map colors based on the Black share of block population.

48

Figure A.2: Share Black residents in school districts, New York metropolitan area, 2020
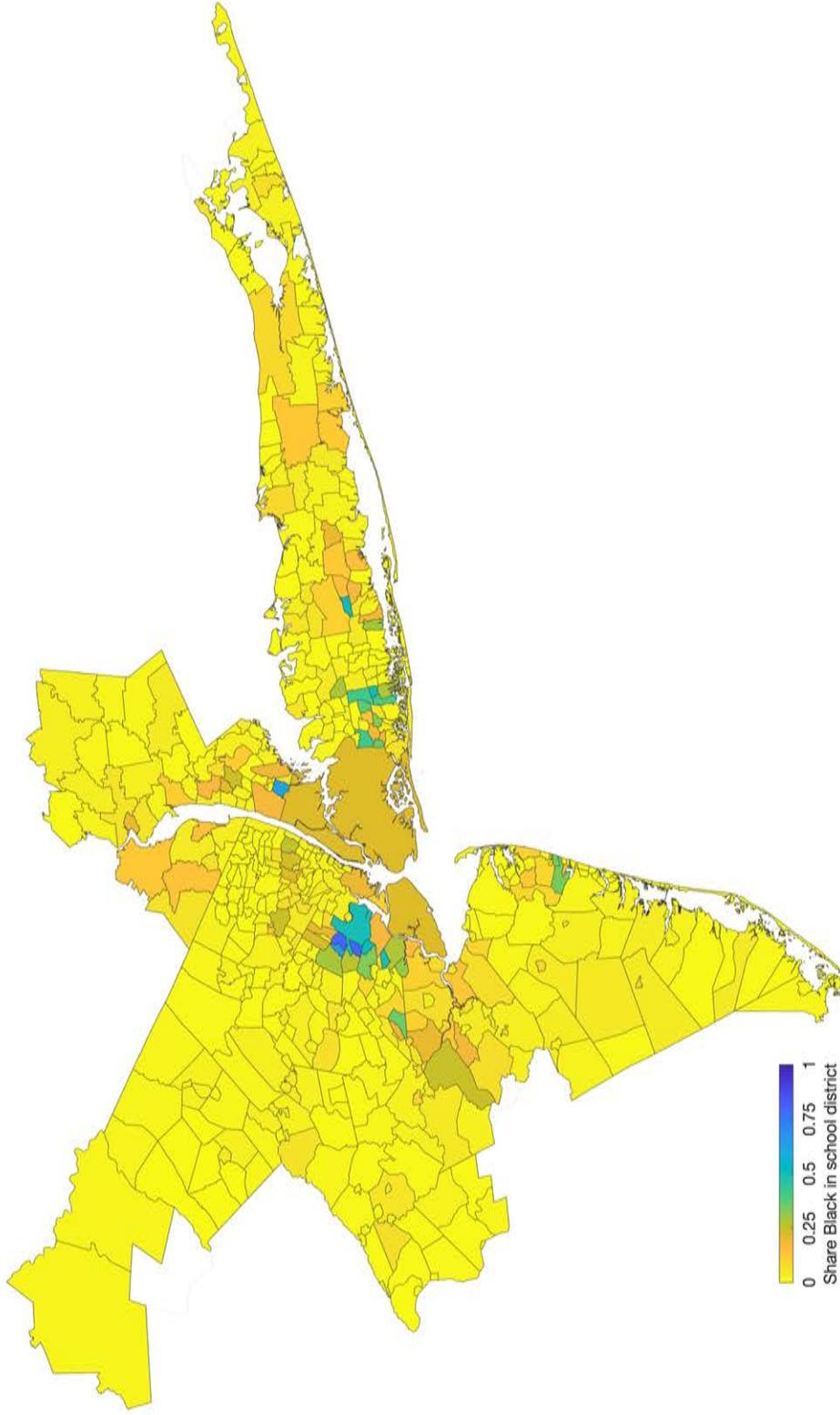
Notes: New York Metropolitan Statistical Area (MSA) and 502 independent school districts (local education agencies) according to 2020 census definitions. Population-weighted scatter plot shows the latitude/longitude location of census block centroids, with colors corresponding to the Black share of block residents. Figure shows a zoomed in section of western Long Island.

Figure A.3: Average metropolitan segregation of minorities, decomposed into between and within school districts, 1990-2020
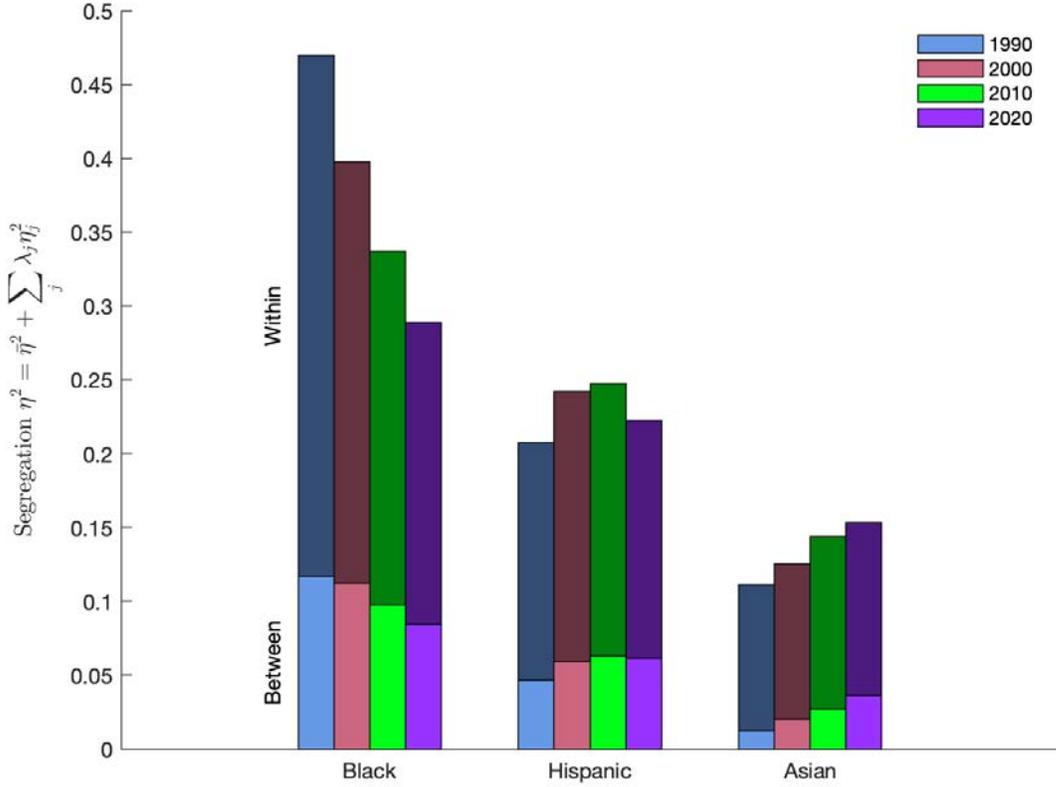
Notes: National average decomposition of total metropolitan segregation of Black, Hispanic, and Asian households. Lighter shade corresponds to between-school district segregation, darker shade to within-district segregation. Estimates based on the variance ratio index, using 1990, 2000, 2010, and 2020 census block data.

Figure A.4: Segregation of minorities, decomposed into between and within school districts, 1990-2020, tract-level measure of segregation
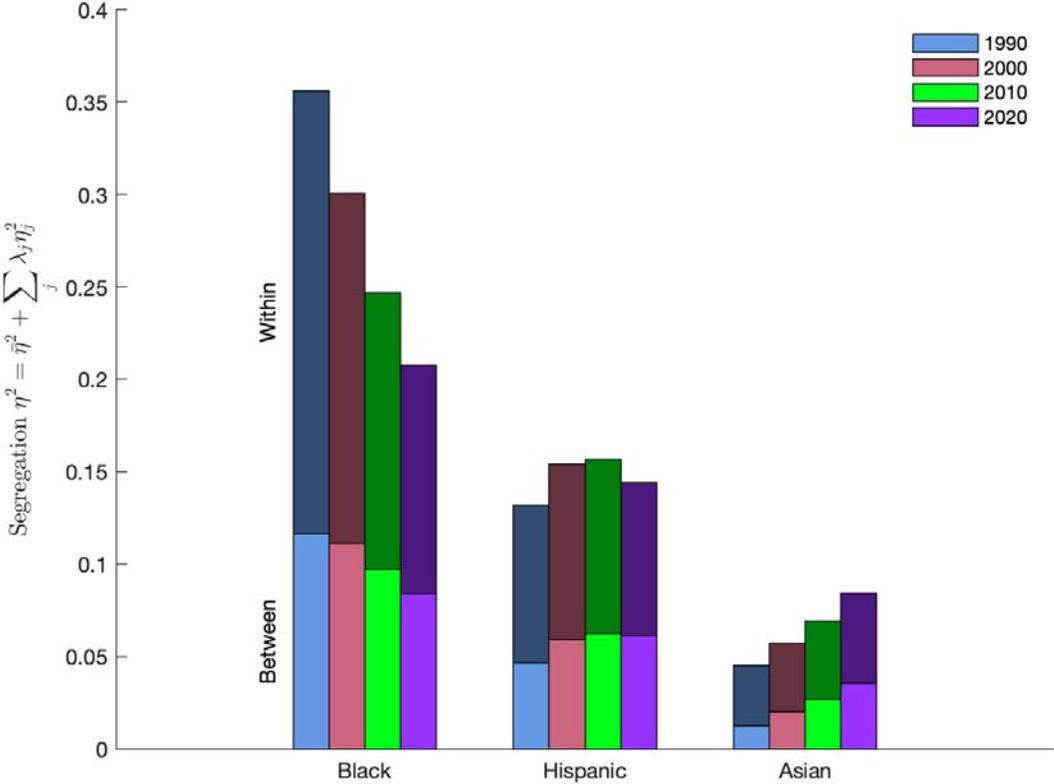
Notes: National average decomposition of total metropolitan segregation of Black, Hispanic, and Asian households. Lighter shade corresponds to between-school district segregation, darker shade to within-district segregation. Estimates based on the variance ratio index, using 1990, 2000, 2010, and 2020 census tract data.

Figure A.5: Metro-area segregation of Hispanic households, 1990-2020
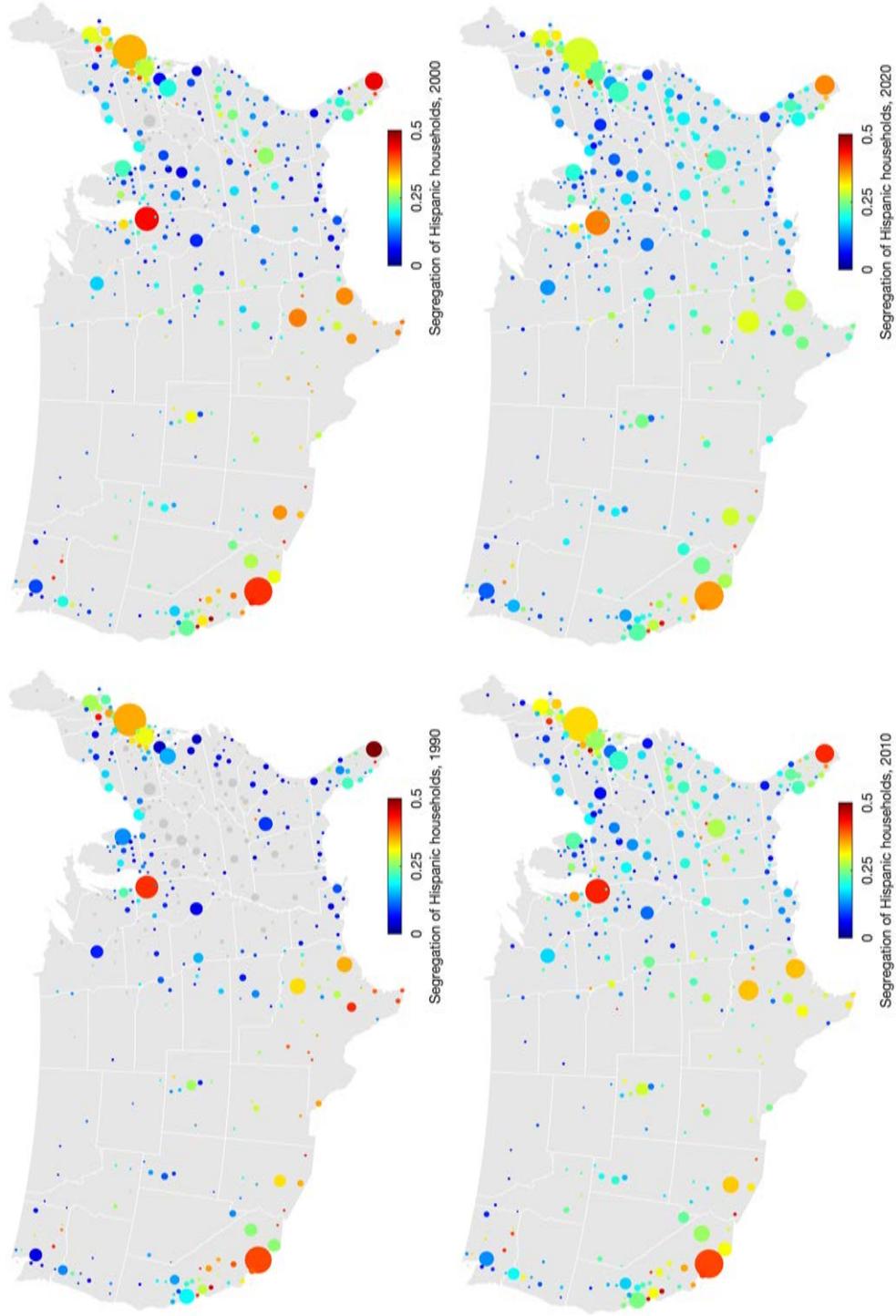
Notes: Location of US metropolitan areas, weighted by population. Heat coloring corresponds to total metropolitan segregation levels for Hispanic residents. Estimates based on the variance ratio index, using 1990, 2000, 2010, and 2020 census block data.

52

Figure A.6: Metro-area segregation of Asian households, 1990–2020
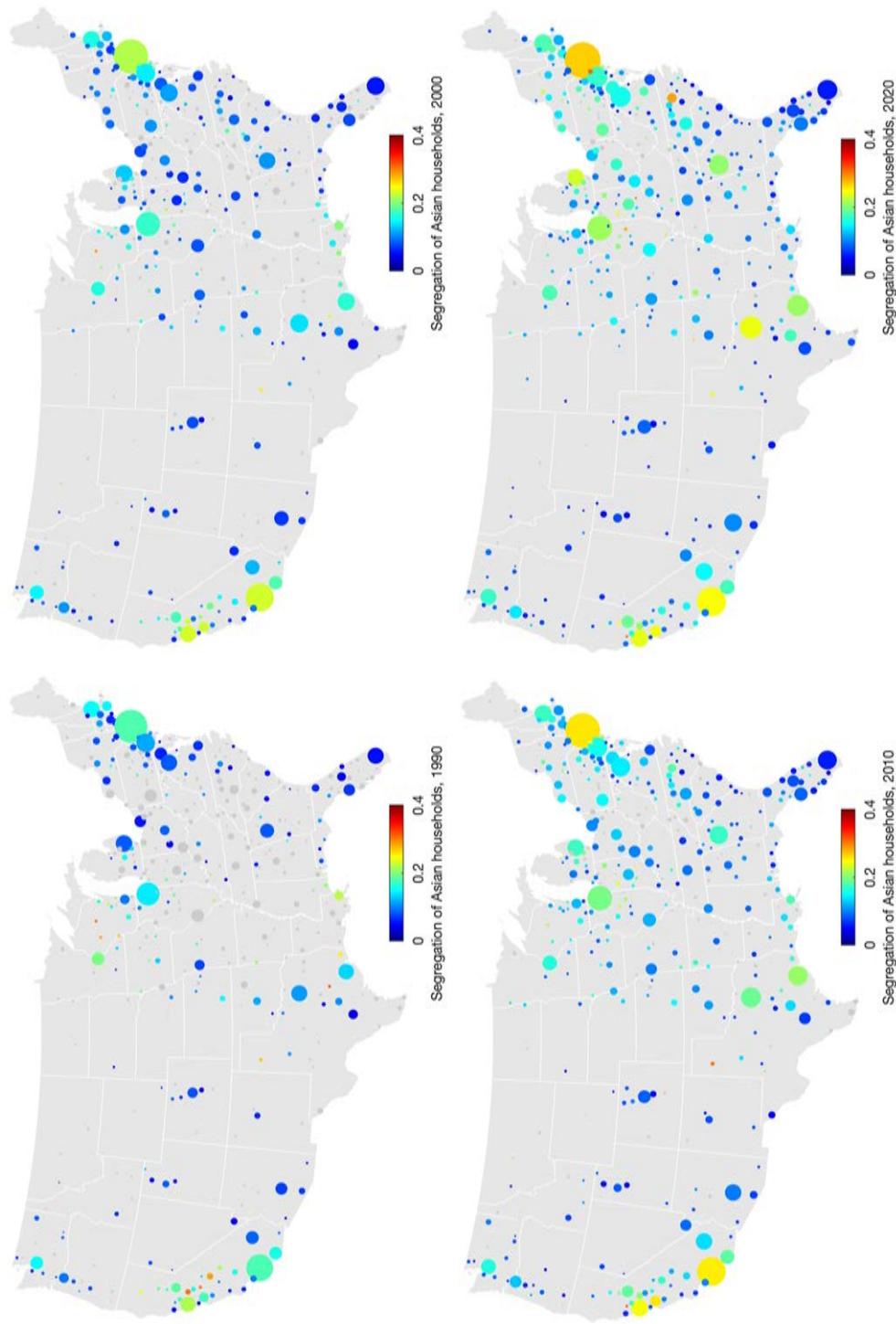
Notes: Location of US metropolitan areas, weighted by population. Heat coloring corresponds to total metropolitan segregation levels for Asian residents. Estimates based on the variance ratio index, using 1990, 2000, 2010, and 2020 census block data.

53

Figure A.7: Evolution of metropolitan segregation decomposition, selected areas, 1990-2020.
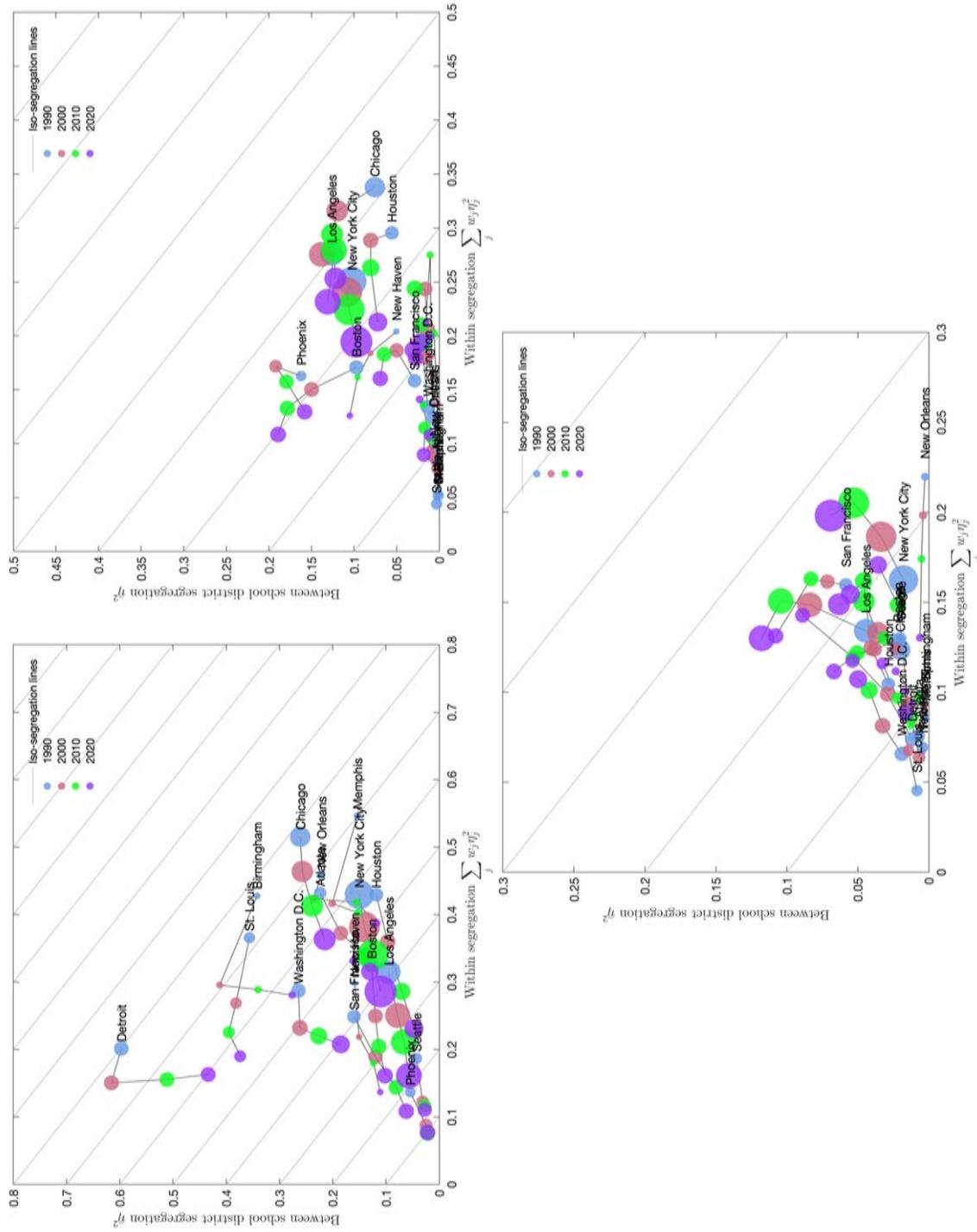
Notes: Population-weighted scatter plot of metropolitan areas, plotting between-district and within-district segregation. Plot colors denote decennial census years. Diagonal lines correspond to an "iso-segregation" locus of equal levels of total segregation.

Figure A.8: Segregation of minorities in 2020 by census region, decomposed into between school districts, between SAZs, and within SAZs, tract-level measure of segregation
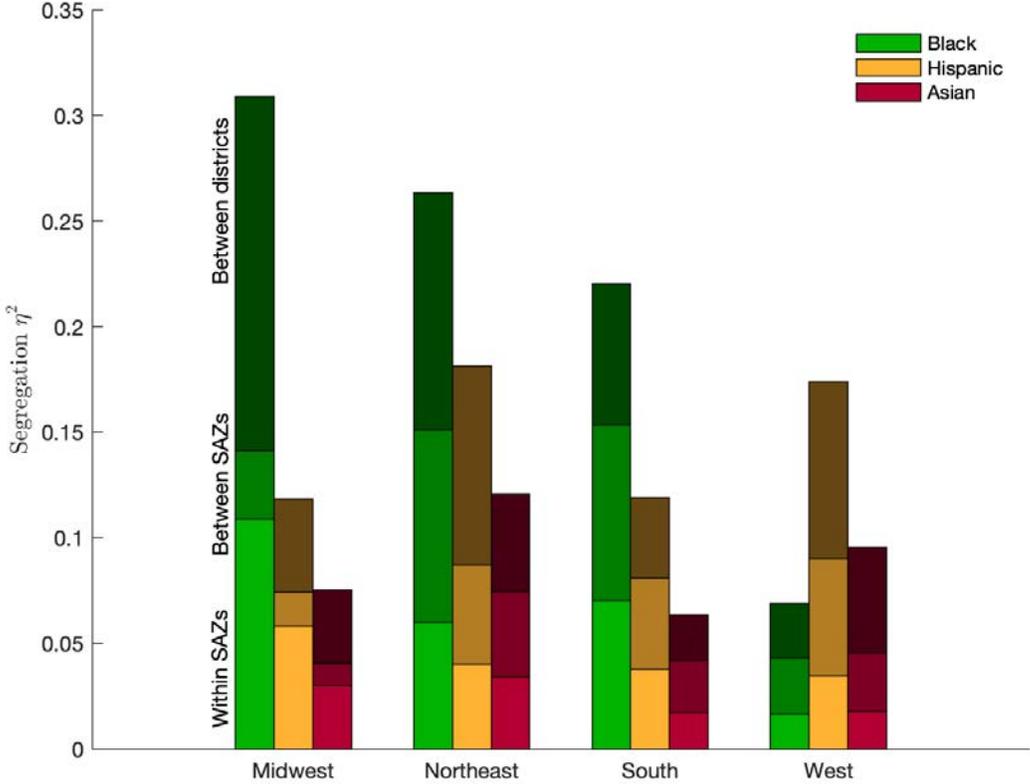
Notes: SAZ = School Attendance Zones. Average metropolitan segregation by US Census region, based on 2020 census tract data. Decomposition terms shown in different color shades, according to the description in Section 4.5.1.

Figure A.9: National average demographic discontinuities at jurisdictional boundaries, by local government type, 2020
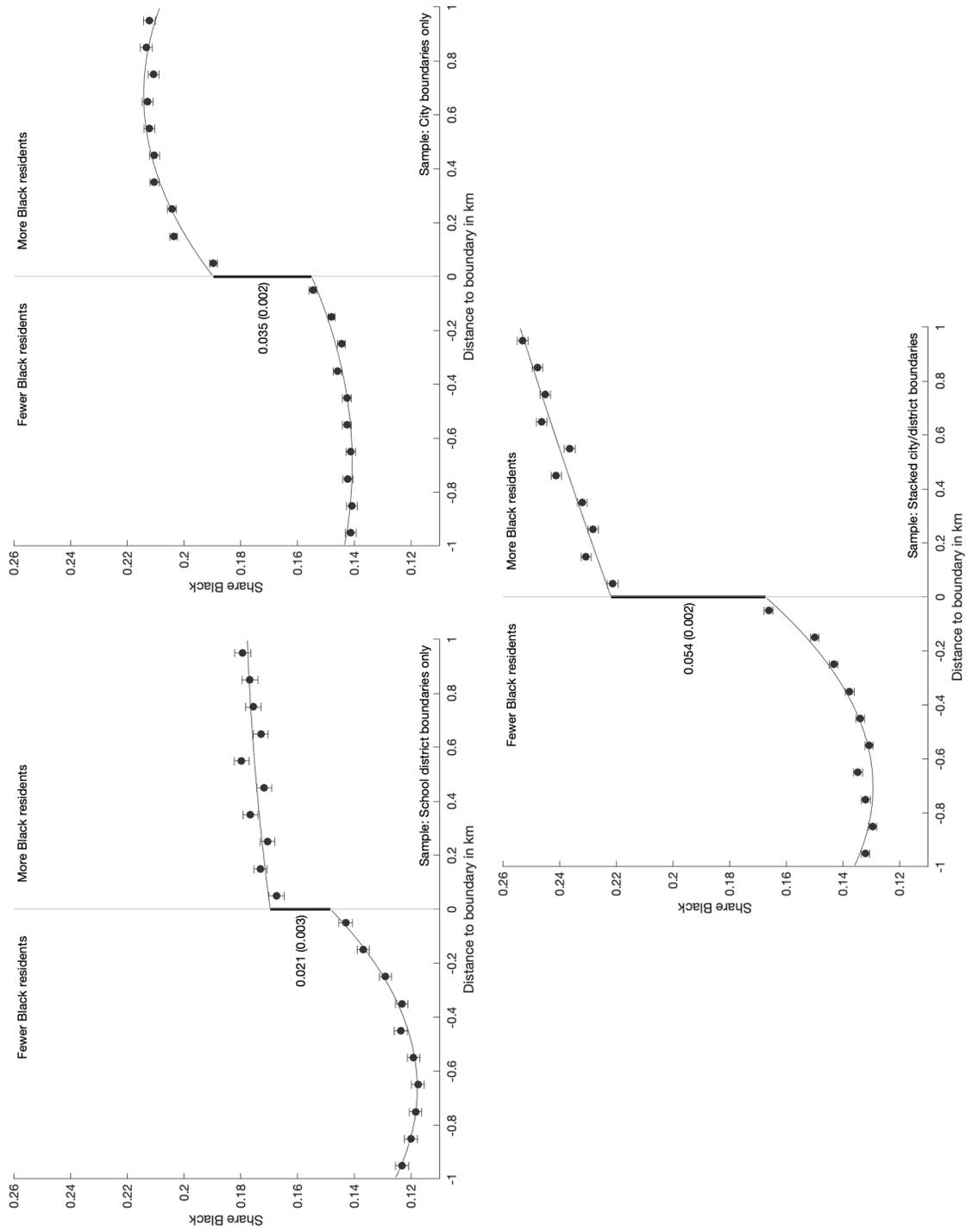
Notes: Spatial regression discontinuity (RD) plots of Black population shares against block distance to jurisdictional boundaries. Horizontal axis measures census blocks' perpendicular centroid distance to jurisdictional boundaries, where negative distance values correspond to the jurisdiction with fewer Black residents. Vertical axis shows the Black share of total census block population in 2020. Scatter plot shows binned means, with bins determined by equally-sized distance steps. Estimation sample is restricted to census blocks within 1 kilometer of a jurisdictional boundary and boundaries with at least one side with 5% Black residents or more, resulting in about 1.5M census blocks across 15,000 boundaries. RD coefficient (along with robust standard error) and quadratic spline fit reported.

Appendix Tables

Table A.1: Average segregation in metro areas, tract-level measure of segregation

	Black				Hispanic				Asian			
	1990	2000	2010	2020	1990	2000	2010	2020	1990	2000	2010	2020
Minority share	0.125	0.129	0.13	0.132	0.101	0.139	0.179	0.203	0.03	0.041	0.053	0.068
Isolation	0.425	0.379	0.334	0.303	0.209	0.26	0.297	0.309	0.072	0.094	0.117	0.144
Segregation	0.356	0.3	0.247	0.207	0.132	0.154	0.157	0.144	0.045	0.057	0.069	0.084
Panel A: County segregation												
Between counties	0.049	0.049	0.044	0.038	0.017	0.02	0.021	0.02	0.005	0.007	0.01	0.013
Within counties	0.307	0.251	0.203	0.17	0.114	0.134	0.136	0.124	0.041	0.05	0.06	0.071
Panel B: City segregation												
Between cities	0.118	0.114	0.1	0.087	0.044	0.055	0.058	0.057	0.012	0.018	0.024	0.032
Within cities	0.238	0.187	0.147	0.12	0.088	0.099	0.099	0.088	0.034	0.039	0.045	0.052
Panel C: School district segregation												
Between school districts	0.116	0.111	0.097	0.084	0.046	0.059	0.062	0.061	0.012	0.02	0.027	0.036
Within school districts	0.24	0.189	0.15	0.123	0.085	0.095	0.094	0.083	0.033	0.037	0.043	0.049
Between SAZs	—	—	—	0.061	—	—	—	0.042	—	—	—	0.026
Within SAZs	—	—	—	0.059	—	—	—	0.046	—	—	—	0.027

Notes: Estimates based on census tract data. Isolation is the mean share of minority group residents, conditional on being a minority. Segregation is the variance ratio index of segregation, an isolation index adjusted for the group's population share. Between-local government segregation decompositions based on the discussion in section 3.5. SAZ = School Attendance Zone. Between-SAZ segregation decomposition based on private data from Precisely for the school year 2020-21.

Table A.2: 20 most segregated and most integrated MAs for Hispanic households, 2020

	2020				Change 1990-2020		
	Rank	m	η^2	$\bar{\eta}^2$	$\bar{\eta}^2/\eta^2$	Δm	$\Delta\eta^2$	$\Delta\bar{\eta}^2$
Panel A: **Most segregated metro areas**								
Reading, PA	1	0.232	0.456	0.36	0.788	4.549	1.26	3.193
Salinas, CA	2	0.605	0.444	0.311	0.701	1.796	0.966	1.117
Santa Cruz-Watsonville, CA	3	0.348	0.408	0.181	0.445	1.71	1.001	1.372
Chicago-Naperville-Elgin, IL-IN-WI	4	0.233	0.375	0.122	0.325	2.125	0.907	1.61
Oxnard-Thousand Oaks-Ventura, CA	5	0.433	0.372	0.216	0.582	1.636	0.95	1.268
Miami-Fort Lauderdale-Pompano Beach, FL	6	0.459	0.369	0.17	0.459	1.649	0.738	0.813
Yakima, WA	7	0.507	0.368	0.181	0.491	2.12	0.865	1.093
Springfield, MA	8	0.195	0.363	0.21	0.578	2.602	0.84	1.869
Los Angeles-Long Beach-Anaheim, CA	9	0.446	0.363	0.131	0.361	1.284	0.902	1.039
Naples-Marco Island, FL	10	0.272	0.345	0	0.001	1.994	0.797	10
Santa Maria-Santa Barbara, CA	11	0.47	0.338	0.167	0.496	1.768	1.066	1.718
Scranton–Wilkes-Barre, PA	12	0.116	0.334	0.129	0.386	20.523	4.658	10
Kennewick-Richland, WA	13	0.335	0.327	0.118	0.362	2.522	0.863	1.068
Allentown-Bethlehem-Easton, PA-NJ	14	0.183	0.324	0.179	0.554	4.342	1	3.683
Providence-Warwick, RI-MA	15	0.141	0.32	0.167	0.523	3.594	1.388	2.264
Trenton-Princeton, NJ	16	0.217	0.318	0.121	0.382	3.598	1.253	2.674
Milwaukee-Waukesha, WI	17	0.116	0.318	0.055	0.172	3.241	1.412	2.911
Bakersfield, CA	18	0.549	0.313	0.205	0.654	1.963	0.791	0.987
Dallas-Fort Worth-Arlington, TX	19	0.293	0.298	0.083	0.279	2.224	0.91	1.734
Boston-Cambridge-Newton, MA-NH	20	0.118	0.298	0.189	0.636	2.558	1.111	1.945
Median of most segregated MAs	10.5	0.282	0.341	0.169	0.475	2.174	0.958	1.726
Panel B: **Most integrated metro areas**								
Bremerton-Silverdale-Port Orchard, WA	165	0.088	0.073	0.006	0.079	2.698	1.838	2.549
Pensacola-Ferry Pass-Brent, FL	164	0.064	0.076	0	0	3.54	1.601	0.064
Olympia-Lacey-Tumwater, WA	163	0.098	0.079	0.005	0.067	3.277	1.628	2.348
Clarksville, TN-KY	162	0.092	0.083	0.017	0.203	3.069	1.51	0.771
Jacksonville, FL	161	0.102	0.086	0.004	0.048	4.165	1.824	6.821
Virginia Beach-Norfolk-Newport News, VA-NC	160	0.075	0.086	0.007	0.083	3.391	2.346	1.932
Spokane-Spokane Valley, WA	159	0.063	0.086	0.004	0.045	3.318	1.213	1.948
Ann Arbor, MI	158	0.056	0.087	0.003	0.039	2.749	1.881	0.679
Palm Bay-Melbourne-Titusville, FL	157	0.112	0.089	0	0	3.643	1.409	10
Kalamazoo-Portage, MI	156	0.056	0.091	0.009	0.102	3.194	1.41	3.667
Fayetteville, NC	155	0.127	0.092	0.007	0.072	3.161	1.594	0.503
Hagerstown-Martinsburg, MD-WV	154	0.059	0.094	0.003	0.029	8.426	1.799	10
Eugene-Springfield, OR	153	0.099	0.094	0.008	0.08	4.066	1.64	10
Albany-Schenectady-Troy, NY	152	0.059	0.097	0.023	0.232	3.95	1.668	4.284
Gainesville, FL	151	0.115	0.097	0.002	0.016	3.369	1.437	0.992
Lansing-East Lansing, MI	150	0.068	0.099	0.023	0.237	1.902	0.992	1.21
Laredo, TX	149	0.952	0.101	0.002	0.023	1.014	0.754	0.111
Tallahassee, FL	148	0.079	0.103	0.004	0.039	3.457	0.982	3.872
Killeen-Temple, TX	147	0.24	0.105	0.007	0.067	1.956	0.772	1.854
Seattle-Tacoma-Bellevue, WA	146	0.112	0.108	0.018	0.168	3.795	2.286	5.78
Median of most integrated MAs	155.5	0.09	0.092	0.006	0.067	3.343	1.598	2.148

Notes: Rank: MA segregation rank out 140 large MAs with at least 5% Hispanic. Changes between 1990-2020 denoted by $\Delta x = x_{2020}/x_{1990}$. Values of 10 and -10 indicate more than ten-fold increases and decreases, respectively.

Table A.3: 20 most segregated and most integrated MAs for Asian households, 2020

			2020				Change 1990-2020	
	Rank	m	η^2	$\bar{\eta}^2$	$\bar{\eta}^2/\eta^2$	Δm	$\Delta\eta^2$	$\Delta\bar{\eta}^2$
Panel A: **Most segregated metro areas**								
Trenton-Princeton, NJ	1	0.126	0.308	0.182	0.589	4.214	3.012	4.996
Raleigh-Cary, NC	2	0.071	0.285	0.015	0.052	4.626	2.709	4.348
New York-Newark-Jersey City, NY-NJ-PA	3	0.125	0.267	0.069	0.258	2.573	1.482	3.872
Los Angeles-Long Beach-Anaheim, CA	4	0.17	0.248	0.118	0.475	1.665	1.388	2.656
San Jose-Sunnyvale-Santa Clara, CA	5	0.384	0.245	0.142	0.581	2.338	1.392	2.279
Dallas-Fort Worth-Arlington, TX	6	0.081	0.243	0.081	0.333	3.408	2.209	8.144
San Francisco-Oakland-Berkeley, CA	7	0.282	0.239	0.108	0.451	1.794	1.097	1.847
Atlantic City-Hammonton, NJ	8	0.081	0.223	0.038	0.172	3.963	2.116	7.308
Chicago-Naperville-Elgin, IL-IN-WI	9	0.072	0.212	0.063	0.298	2.357	1.475	3.141
Fayetteville-Springdale-Rogers, AR	10	0.057	0.211	0.023	0.107	8.579	2.099	7.696
Houston-The Woodlands-Sugar Land, TX	11	0.084	0.21	0.055	0.263	2.491	1.578	1.94
Stockton, CA	12	0.186	0.208	0.042	0.201	1.602	0.685	1.218
Atlanta-Sandy Springs-Alpharetta, GA	13	0.066	0.207	0.036	0.173	3.986	2.493	4.997
Ann Arbor, MI	14	0.091	0.194	0.056	0.286	2.217	1.439	2.716
Sacramento-Roseville-Folsom, CA	15	0.158	0.192	0.073	0.378	2.134	1.026	1.726
Harrisburg-Carlisle, PA	16	0.053	0.184	0.03	0.161	4.823	2.106	9.865
Boston-Cambridge-Newton, MA-NH	17	0.087	0.178	0.067	0.375	3.063	1.181	3.045
Minneapolis-St. Paul-Bloomington, MN-WI	18	0.072	0.178	0.041	0.228	2.904	0.903	2.66
Austin-Round Rock-Georgetown, TX	19	0.072	0.176	0.032	0.182	3.328	1.685	6.136
San Diego-Chula Vista-Carlsbad, CA	20	0.129	0.176	0.04	0.228	1.743	1.106	1.766
Median of most segregated MAs	10.5	0.086	0.21	0.055	0.261	2.738	1.478	3.093
Panel B: **Most integrated metro areas**								
Reno, NV	47	0.066	0.067	0	0.004	1.823	0.863	1.738
Bremerton-Silverdale-Port Orchard, WA	46	0.063	0.069	0.009	0.125	1.575	1.286	1.352
Bridgeport-Stamford-Norwalk, CT	45	0.054	0.073	0.008	0.114	2.659	1.043	2.399
Salt Lake City, UT	44	0.059	0.079	0.005	0.063	2.238	0.927	0.923
Boulder, CO	43	0.051	0.088	0.003	0.032	2.098	1.213	0.938
Olympia-Lacey-Tumwater, WA	42	0.07	0.088	0.017	0.192	1.937	1.049	1.474
Salinas, CA	41	0.066	0.093	0.024	0.254	0.919	0.88	0.991
Santa Rosa-Petaluma, CA	40	0.05	0.095	0.012	0.123	1.914	1.984	1.919
Oxnard-Thousand Oaks-Ventura, CA	39	0.079	0.098	0.016	0.164	1.617	0.989	3.522
Las Vegas-Henderson-Paradise, NV	38	0.114	0.102	0	0	3.452	2.091	∞
Modesto, CA	37	0.071	0.107	0.014	0.135	1.442	0.683	1.001
Gainesville, FL	36	0.055	0.125	0.01	0.078	2.596	1.171	3.341
College Station-Bryan, TX	35	0.057	0.131	0.03	0.226	2.004	0.413	1.268
Albany-Schenectady-Troy, NY	34	0.052	0.132	0.029	0.221	4.104	1.626	3.459
Merced, CA	33	0.077	0.138	0.035	0.254	0.971	0.457	0.897
Portland-Vancouver-Hillsboro, OR-WA	32	0.077	0.141	0.029	0.203	2.304	1.461	2.699
Santa Maria-Santa Barbara, CA	31	0.061	0.143	0.036	0.249	1.493	2.158	3.201
Riverside-San Bernardino-Ontario, CA	30	0.08	0.15	0.047	0.315	2.216	1.708	4.434
Bakersfield, CA	29	0.053	0.152	0.044	0.29	1.94	0.936	0.956
Vallejo, CA	28	0.17	0.155	0.03	0.192	1.426	0.884	0.608
Median of most integrated MAs	37.5	0.064	0.104	0.016	0.178	1.939	1.046	1.413

Notes: Rank: MA segregation rank out 140 large MAs with at least 5% Asian. Changes between 1990-2020 denoted by $\Delta x = x_{2020}/x_{1990}$. Values of 10 and -10 indicate more than ten-fold increases and decreases, respectively.